**University of Alberta**

# Fine coal cleaning using an air dense medium fluidized bed

by

Carol Ka Yee Mak

A thesis submitted to the Faculty of Graduate Studies and Research
in partial fulfillment of the requirements for the degree of

Master of Science
In
Materials Engineering

Department of Chemical and Materials Engineering

Edmonton, Alberta
Spring 2007

Library and Archives Canada
Published Heritage Branch
395 Wellington Street
Ottawa ON K1A 0N4
Canada

Bibliothèque et Archives Canada
Direction du Patrimoine de l'édition
395, rue Wellington
Ottawa ON K1A 0N4
Canada

*Your file Votre référence*
*ISBN: 978-0-494-29993-7*
*Our file Notre référence*
*ISBN: 978-0-494-29993-7*

NOTICE:
The author has granted a non-exclusive license allowing Library and Archives Canada to reproduce, publish, archive, preserve, conserve, communicate to the public by telecommunication or on the Internet, loan, distribute and sell theses worldwide, for commercial or non-commercial purposes, in microform, paper, electronic and/or any other formats.

The author retains copyright ownership and moral rights in this thesis. Neither the thesis nor substantial extracts from it may be printed or otherwise reproduced without the author's permission.

AVIS:
L'auteur a accordé une licence non exclusive permettant à la Bibliothèque et Archives Canada de reproduire, publier, archiver, sauvegarder, conserver, transmettre au public par télécommunication ou par l'Internet, prêter, distribuer et vendre des thèses partout dans le monde, à des fins commerciales ou autres, sur support microforme, papier, électronique et/ou autres formats.

L'auteur conserve la propriété du droit d'auteur et des droits moraux qui protège cette thèse. Ni la thèse ni des extraits substantiels de celle-ci ne doivent être imprimés ou autrement reproduits sans son autorisation.

---

In compliance with the Canadian Privacy Act some supporting forms may have been removed from this thesis.

While these forms may be included in the document page count, their removal does not represent any loss of content from the thesis.

Conformément à la loi canadienne sur la protection de la vie privée, quelques formulaires secondaires ont été enlevés de cette thèse.

Bien que ces formulaires aient inclus dans la pagination, il n'y aura aucun contenu manquant.

Canada

*For my family, friends and dog Lufi.*

## ABSTRACT

An air dense medium fluidized bed separator for dry coal cleaning may benefit the coal industry by removing the ash-forming mineral matters along with associated environmentally harmful toxic metals in an economical way. Exploratory testing on an Alberta sub-bituminous coal was conducted with a 5-cm and a 20-cm diameter fluidized bed. Operating in a batch mode, the effect of medium particle size, coal size and fluidization air velocity on separation efficiency was evaluated. It was found that the bubbling fluidized bed formed with solids that belong to Geldart B classification was most suitable for coal separation. Separation efficiency of this method was poor for 1.00 mm and finer coal. It was found that mercury content and ash content were correlated for the coal used in this study, and coal cleaning could be considered as a potential approach for mercury emission control from coal-fired power plants.

**ACKNOWLEDGEMENTS**

I would like to thank my supervisor Dr. Zhenghe Xu for his guidance, patience and encouragement throughout the course of this thesis.

My gratitude also extends to the Advanced Coal Cleaning and Combustion Technology research group, Oil Sands research group, and the staff in the Department of Chemical and Materials Engineering at the University of Alberta.

I would like to thank Mr. Riley Beauchamp in the Department of Chemical and Materials Engineering at the University of Alberta for conducting the mercury analysis.

Finally, I would like to thank the NSERC/EPCOR/AERI Industrial Research Chair for the financial support that made this thesis project possible.

**TABLE OF CONTENTS**

**CHAPTER 1 INTRODUCTION** ..... **1**

**CHAPTER 2 LITERATURE REVIEW** ..... **5**

*2.1 Gas-solid fluidized bed* ..... *6*

*2.2 Use of ADMFB for coal cleaning* ..... *11*

*2.3 Association of mercury with mineral matters in coal* ..... *12*

**CHAPTER 3 MATERIALS AND EXPERIMENTAL SETUP** ..... **15**

*3.1 Materials* ..... *15*

3.1.1 Media particles ..... 15

3.1.2 Coal ..... 15

*3.2 Experimental setup* ..... *16*

3.2.1 Process schematics ..... 16

3.2.2 Operation procedure ..... 17

*3.3 Analyses* ..... *19*

3.3.1 Particle size distribution ..... 19

3.3.2 Density ..... 20

3.3.3 Ashing ..... 20

3.3.4 Float-sink test ..... 21

3.3.5 Mercury ..... 22

**CHAPTER 4 ADMFB EXPERIMENTS WITH A 5-CM DIAMETER SEPARATOR** ..... **23**

*4.1 Float-sink analysis of Seam 1 and Seam 2 coal* ..... *24*

*4.2 Fluidization classification of medium particles and coal* ..... *26*

*4.3 Parameters investigation* ..... *29*

4.3.1 Fluidized bed characterization ..... 31

4.3.2 Effect of medium particle size on ADMFB separation ..... 36

4.3.3 Effect of coal size (lower separation limit) on ADMFB separation ..... 40

4.3.4 Comparison of ADMFB and pneumatic separation ..... 42

*4.4 Summary* ..... *44*

**CHAPTER 5 ADMFB EXPERIMENTS WITH A 20-CM DIAMETER SEPARATOR – PARAMETERS OPTIMIZATION** ..... **46**

*5.1 Fluidized bed characterization* ..... *48*

*5.2 Effect of fluidization air velocity on ADMFB separation* ..... *51*

*5.3 Estimate of medium particle size during optimal fluidization* ..... *62*

*5.4 Separation efficiency evaluated at optimal fluidization air velocity* ..... *65*

*5.5 Effect of coal loading on ADMFB separation* ..... *70*

*5.6 Effect of coal size on ADMFB separation* ..... *75*

*5.7 Effect of bed height and fluidization duration on ADMFB separation* ..... *79*

*5.8 Summary* ..... *84*

**CHAPTER 6 ASSOCIATION OF MERCURY AND MINERAL MATTERS IN COAL** ..... **85**

**CHAPTER 7 CONCLUSIONS** ..... **89**

**CHAPTER 8 RECOMMENDATIONS** ..... **90**

**REFERENCES** ..... **91**

**APPENDICES** ..... **97**

*Appendix A* ..... *97*

*Appendix B* ..... *101*

*Appendix C* ..... *103*

*Appendix D* ..... *104*

*Appendix E* ..... *105*

**LIST OF TABLES**


Table 4-1. Size-by-size ash content (%) of Seam 1 and Seam 2 coal. ..... 26

Table 4-2. Physical properties and fluidization characteristics of media tested with 5-cm diameter ADMFB separator at 1.0 cm packed bed height. ..... 35

Table 5-1. Physical properties of media used in a 20-cm diameter ADMFB separator. 48

Table 5-2. Fluidization characteristics of media in a 20-cm diameter ADMFB separator at packed bed heights of 8 cm and 15 cm. ..... 51

Table 5-3. Size distribution of coal particles used for ADMFB experiment with a 20-cm diameter ADMFB separator. ..... 52

Table 5-4. Optimal fluidization air velocity for ADMFB separation in a 20-cm diameter separator with medium particles at a packed bed height of 15 cm. ..... 60

Table 5-5. Optimal fluidized bed height for ADMFB separation in a 20-cm diameter separator with medium particles at a packed bed height of 15 cm. ..... 60

Table 5-6. Yield and ash contents of cleaned coal samples collected in ADMFB separation experiments ..... 66

Table 5-7. Separation efficiency of a 20-cm diameter ADMFB separator with Seam 2 coal. ..... 68

Table B-1. Values used for calculation of $u_{mf}$ using a 20-cm diameter ADMFB separator. ..... 101

Table C-1. Float-sink analysis of feed and cleaned coal in 22.6x5.66 mm size fraction. ..... 103

Table D-1. Values used for calculation of $E_p$ of a cleaned coal sample in 22.6x5.66 mm size fraction.....104

Table E-1. Values used for calculation of ash rejection, mercury rejection and combustible recovery of a cleaned coal sample in 22.6x5.66 mm size fraction. .....105

**LIST OF FIGURES**

Figure 3-1. Process diagram of the air dense medium fluidized bed separator. ..... 16

Figure 4-1. Float-sink analysis of crushed Seam 1 coal. ..... 24

Figure 4-2. Float-sink analysis of crushed Seam 2 coal. ..... 25

Figure 4-3. Fluidization classification diagram (Geldart, 1973). ..... 28

Figure 4-4. A photo of the 5-cm diameter ADMFB separation device. ..... 29

Figure 4-5. Fluidized bed height measurements: (a) Packed bed height, (b) Fluidized base height and (c) Fluidized peak height..... 30

Figure 4-6. Snapshots of the packed bed (left) and fluidized bed (right): (a) Packed bed height, (b) Fluidized base height and (c) Fluidized peak height..... 31

Figure 4-7. Effect of fluidization air velocity on bed height with a 5-cm diameter ADMFB separator and magnetite particles in two different size fractions. 33

Figure 4-8. Effect of fluidization air velocity on bed height with a 5-cm diameter ADMFB separator and coal particles in two different size fractions..... 33

Figure 4-9. Schematic drawing of bed expansion during fluidization: a) Finer medium particles and b) Coarser medium particles..... 37

Figure 4-10. Effect of magnetite particle size on separation of coal in 3.36x1.00 mm size fraction. ..... 38

Figure 4-11. Effect of magnetite particle size on separation of coal in 1.00x0.42 mm size fraction. ..... 41

Figure 4-12. Comparison of ADMFB and pneumatic methods on separation of coal in 3.36x1.00 mm size fraction..... 43

Figure 5-1. Particle size distributions of media. ..... 47

Figure 5-2. Effect of fluidization air velocity on bed height of Medium A in a 20-cm diameter ADMFB separator..... 49

Figure 5-3. Effect of fluidization air velocity on bed height of Medium B in a 20-cm diameter ADMFB separator..... 49

Figure 5-4. Effect of fluidization air velocity on bed height of Medium C in a 20-cm diameter ADMFB separator..... 50

Figure 5-5. Effect of fluidization air velocity on ADMFB separation of coal in 22.6x5.66 mm size fraction with Medium B as separation medium. ..... 53

Figure 5-6. Effect of fluidization air velocity on ADMFB separation of coal in 5.66x3.36 mm size fraction with Medium B as separation medium. ..... 53

Figure 5-7. Effect of fluidization air velocity on ADMFB separation of coal in 3.36x1.00 mm size fraction with Medium B as separation medium. ..... 54

Figure 5-8. Effect of fluidization air velocity on ADMFB separation of coal in 3.36x1.00 mm size fraction with Medium A as separation medium. ..... 56

Figure 5-9. Effect of fluidization air velocity on ADMFB separation of coal in 3.36x1.00 mm size fraction with Medium C as separation medium. ..... 58

Figure 5-10. Median sizes of Medium A particles at various heights during fluidization. .. ..... 63

Figure 5-11. Median sizes of Medium B particles at various heights during fluidization. .. ..... 64

Figure 5-12. Median sizes of Medium C particles at various heights during fluidization. .. ..... 64

Figure 5-13. Partition curve for cleaned coal samples obtained using Medium B at optimal fluidization air velocity. Please refer to Appendix C for sample calculation. ..... 67

Figure 5-14. Effect of coal loading on ADMFB separation coal in 22.6x5.66 mm size fraction using Medium B. ..... 71

Figure 5-15. Effect of coal loading on ADMFB separation of coal in 5.66x3.36 mm size fraction using Medium B. ..... 71

Figure 5-16. Effect of the coal loading on ADMFB separation of coal in 3.36x1.00 mm size fraction using Medium B. ..... 72

Figure 5-17. Effect of volume of coal added on ADMFB separation of coal in 3.36x1.00 mm size fraction using Medium A ..... 73

Figure 5-18. Effect of volume of coal added on ADMFB separation of coal in 3.36x1.00 mm size fraction using Medium C. ..... 74

Figure 5-19. Effect of size fraction of coal added on ADMFB separation of coal in 22.6x5.66 mm size fraction using Medium B. ..... 77

Figure 5-20. Effect of size fraction of coal added on ADMFB separation of coal in 3.36x1.00 mm size fraction using Medium B. ..... 77

Figure 5-21. Effects of packed bed height and fluidization duration on ADMFB separation of coal in 3.36x1.00 mm size fraction using Medium A. ..... 80

Figure 5-22. Effects of packed bed height and fluidization duration on ADMFB separation of coal in 3.36x1.00 mm size fraction using Medium B. ..... 81

Figure 5-23. Effects of packed bed height and fluidization duration on ADMFB separation of coal in 3.36x1.00 mm size fraction using Medium C. ..... 81

Figure 5-24. Ash content of coal particles in medium particles under optimal separation at 15-cm packed bed height and 15 min of fluidization duration. ..... 83

Figure 6-1. Relationship between ash content and mercury content for Seam 1 coal..... 85

Figure 6-2. Relationship between ash content and mercury content for Seam 2 coal..... 86

Figure 6-3. Correlation between ash rejection and mercury rejection for Seam 2 coal. Please see Appendix E for sample calculation. ..... 87

## LIST OF NOMENCLATURES

| | |
|---|---|
| $Ar$ | Archimedes number, dimensionless |
| $d_p$ | Geometric diameter based on screen analysis, μm |
| $d_{pi}$ | Mean particle diameter of particles in a certain size fraction, μm |
| $g$ | Acceleration of gravity, 9.81 m/s$^2$, |
| $h_{mb}$ | Minimum bubbling bed height, cm |
| $h_{optimal}$ | Optimal bubbling bed height, cm |
| $Re_{p,mf}$ | Reynolds number of particles at minimum fluidizing conditions, dimensionless |
| $S.G.$ | Specific gravity, dimensionless |
| $u$ | Mean gas velocity, m/s |
| $u_{cf}$ | Complete fluidization air velocity, cm/s |
| $u_{mb}$ | Minimum bubbling velocity, cm/s |
| $u_{mf}$ | Superficial gas velocity at minimum fluidization conditions, cm/s |
| $u_{mfi}$ | Superficial gas velocity at minimum fluidization conditions of particles in a certain size fraction, cm/s |
| $u_{optimal}$ | Superficial gas velocity at optimal fluidization conditions of particles in a certain size fraction, cm/s |
| $x_i$ | Weight fraction of particles in a certain size fraction, dimensionless |
| $\varepsilon_{mf}$ | Void fraction at minimum fluidizing conditions, dimensionless |
| $\mu$ | Viscosity of gas, kg/m·s |
| $\rho_{50}$ | Separation density (also known as partition or equal errors density) |

| | |
|---|---|
| $\rho_f$ | Gas density, kg/m$^3$ |
| $\rho_g$ | Gas density, kg/m$^3$ |
| $\rho_s$ | Solid density, kg/m$^3$ |
| $\phi_s$ | Sphericity of a particle, dimensionless |

# CHAPTER 1 INTRODUCTION

Coal is second only to oil in meeting today's world energy needs and is a critical ingredient in the manufacture of steel. Combustion of fossil fuels currently dominates world energy production and will continue to do so in the foreseeable future. As a result of industries' negligence in emission control practices in the past, coal combustion is perceived as a major environmental pollution source.

Greenhouse gas emissions from coal-fired power plants will greatly exceed the cutbacks promised by nations that have signed the Kyoto Protocol. Evidence suggests that greenhouse gases emitted from human activities contribute to the recent abrupt climate changes around the world. Efforts have been focused on seeking out and commercializing alternative resources such as wind, solar and biomass for electricity production. Even though these new routes for electricity production promise lower environmental impact, they are not widely accepted due to reasons such as high installation cost, limited availability of resources and the infancy of the technology compared to existing routes for electricity production. Since there is a lack of promising alternative route for electricity production, attention has been placed on making coal usage for electricity production more environmentally friendly.

The release of trace toxic metals during coal combustion has been targeted for emission control due to their detrimental effects on human health. A number of studies have been devoted to investigations of the toxicity of heavy metals released during coal combustion to different biological organs or systems such as the liver, kidneys, and hemopoietic and reproductive nerve and immune systems (Goyer, 1991). Among the

heavy metals examined, mercury has been identified to have persistent bio-toxicity due to its high volatility and bio-accumulative nature. For this reason, mercury has been specifically targeted for emission control for coal-fired plants.

In Alberta, the current practice is to directly burn as-mined coal for electricity production. As-mined coal is a composite of carbon, other organic matters and ash-forming mineral matters. In addition to greenhouse gas generation from the combustion of carbon, burning as-mined coal generates additional air pollutants due to the presence of mineral matters. Coal cleaning is a process used to liberate and separate the mineral matters from the carbon-rich phase in as-mined coal. Even though it is still not generally practiced by the power industry, coal cleaning is getting more recognition for its role in decreasing the environmental impact of burning coal. The extent of mineral matter removal depends on the characteristics of the coal and the efficiency of the cleaning process. Removal of mineral matters is anticipated to contribute to the reduction in emission of air toxics.

Coal cleaning has been practiced for more than a century. Most of the widely used unit operations for rejecting mineral matters are water-based, such as froth flotation, dense medium separation and hydraulic concentrations. These methods have shown some degree of success in some applications. However, general acceptance of these methods by the coal industry is not recognized, mainly because of economic constraints from de-watering of fine coal products. In some cases where there are significant regional limitations, such as cold weather in Alberta or aridity in northwest China, these wet cleaning methods become unfeasible. As such, dry coal cleaning methods are more appealing. Although there are some inherent drawbacks such as dust handling and

potential explosion risks, dry coal beneficiation provides considerable incentives, such as lower capital investment and lower operating cost than most wet cleaning strategies.

Dry coal cleaning generally exploits the differences of constitutes in hardness, shape, coefficient of friction and specific gravity (*S.G.*). Compared with wet cleaning processes, the separation efficiency of dry coal cleaning is generally low. Over the last few decades, extensive research has been devoted to the development of a dry beneficiation technology featuring high separation efficiency with fewer economic and engineering constraints. One of the significant advances has been in utilizing an air dense medium fluidized bed (ADMFB) to efficiently beneficiate coarse coals (50 x 6 mm). In 1994, the first ADMFB plant was commercialized in China to beneficiate bituminous coal (Luo et al., 2003b). This advanced method has drawn great attention from coal processors, especially those who encounters difficulties with wet separation process due to water shortages and/or easily slimed nature of coal. Sub-bituminous and lower rank coals are easily slimed when processed using wet separation methods. ADMFB is an attractive technology for cleaning Alberta's sub-bituminous coal, but exploratory work on this topic has not been established in literature yet.

The objective of this thesis is to evaluate the applicability of using ADMFB separation for cleaning an Alberta sub-bituminous coal. The potential of using ADMFB separation for mercury removal from this coal is also investigated. In Chapter 2, a literature review on gas-solid fluidized beds and the usage of ADMFB for coal cleaning are presented. Chapter 3 provides the details on materials and experimental setup for ADMFB separation. Analyses performed to interpret experimental results are also covered in this chapter. Experimental results and discussion are the main subjects of

Chapters 4, 5 and 6. Characteristics of the ADMFB process are investigated with a 5-cm diameter separator, and the results are presented in Chapter 4. In Chapter 5, the results from the parameter optimization study with a 20-cm diameter separator are discussed. The results from the preliminary study on the association of mercury and mineral matters in the sub-bituminous coal studied are presented in Chapter 6. Conclusions and recommendations are given in Chapters 7 and 8, respectively.

# CHAPTER 2 LITERATURE REVIEW

Fluidization is an operation by which solid particles are transformed into a fluid-like state through suspension in a gas or liquid. Existing industrial applications of fluidized beds include coal gasification, coal de-volatilization, pneumatic transport, catalytic synthesis, metallurgical processes, coating of objects and agricultural heat exchange processes. In liquid-solid systems, an increase in the flow rate of liquid above minimum fluidization usually results in a smooth and progressive expansion of the bed. Macroscopic flow instabilities are damped and remain small, and the heterogeneity of the liquid-solid suspension is not observed under normal conditions (Kunii and Levenspiel, 1991). In contrast, gas-solid systems behave erratically as a result of the compressible nature of gases, causing large instabilities in solid particles as the fluidization gas velocity ($u$) increases.

A gas-solid fluidized bed exhibits liquid-like behaviour. When large and low-density objects are pushed into a gas-solid fluidized bed, these objects will pop up and float on the top of the bed. This property is what motivates the utilization of a gas-solid fluidized bed as a dry process for coal cleaning. In as-mined coal, mineral matters usually have a higher density than the carbon-rich phase. By forming a gas-solid fluidized bed with an intermediate density, mineral matters will sink while the carbon-rich phase will float. Despite wide industrial usage and extensive research efforts, there is no adequate model to describe gas-solid fluidization systems because the degrees of freedom in these systems are too numerous (Geldart, 1986).

## 2.1 *Gas-solid fluidized bed*

The onset of fluidization occurs when all the particles are just suspended by the upward flowing gas. In this thesis research, this bed is considered to be just fluidized and is referred to as a bed at minimum fluidization. The corresponding fluidization gas velocity is referred to as the minimum fluidization gas velocity ($u_{mf}$). Since minimum fluidization occurs when all the particles are just suspended by the upward flowing gas, existing equations to calculate $u_{mf}$ are derived from the state when the drag force from the upward moving gas equals the weight of particles. Following is the equation reported by Kunii and Levenspiel (1991) and most commonly used to predict $u_{mf}$ for fine particles:

$$u_{mf} = \frac{d_p^2(\rho_s - \rho_g)g}{150\mu} \frac{\varepsilon_{mf}^3 \phi_s^2}{1-\varepsilon_{mf}}, \quad \mathrm{Re}_{p,mf} < 20 \tag{2.1}$$

where $Re_{p,\,mf}$ and $Ar$ are given by

$$\mathrm{Re}_{p,mf} = [(33.7)^2 + 0.0408 Ar]^{1/2} - 33.7 \tag{2.2}$$

$$Ar = \frac{d_p^3 \rho_g (\rho_s - \rho_g) g}{\mu^2} \tag{2.3}$$

For particles of a given size distribution, the following equation is used to estimate $d_p$:

$$d_p = \frac{1}{\Sigma(x_i / d_{pi})} \tag{2.4}$$

It has been well documented that $u_{mf}$ changes with experimental parameters such as operating gas pressure (Marzocchella and Salatino, 2000) and bed height (Delebarre et al., 2004). Nonetheless, Equation 2.1 is still a simple way to estimate $u_{mf}$ when experimental data is unavailable.

For solids having a wide size distribution and large mean diameter, segregation by size tends to occur at fluidization gas velocity close to $u_{mf}$ of the mixture. Knowlton (1974) defined the term complete fluidization gas velocity ($u_{cf}$) as the velocity at which all the particles are fully supported (with segregation) and proposed that:

$$u_{cf} = \Sigma x_i u_{mfi} \tag{2.5}$$

Even though discussions of the so-called minimum fluidization velocity and complete fluidization velocity are numerous in literature, the definition and interpretation of $u_{mf}$ have been widely varied (Delebarre et al., 1994).

In a gas-solid fluidized bed, bed expansion occurs, apparently smoothly and homogenously, until a velocity is reached at which small bubbles appear at the surface. The average of the two experimental velocities at which bubbles appear and disappear is called the minimum bubbling velocity ($u_{mb}$).

By carefully observing the fluidization of a wide range of types and sizes of solids, Geldart (1973) came up with four kinds of clearly distinguishable particle behaviours. These kinds of behaviours are divided into groups. From the smallest to the largest particles:

- Group C: cohesive or very fine particles. Normal fluidization is extremely difficult for this group of solids because inter-particle forces are greater than those resulting from the action of gas. Cosmetic particles, flour and starch are typical of this kind of solid.
- Group A: aeratable, or materials having a small mean particle size and/or low particle density (<~1.4 g/cm$^3$). These solids fluidize easily, with smooth fluidization at low gas velocities and controlled bubbling with small bubbles at

higher gas velocities. Face centred cubic catalyst particles are representative of this kind of solid.

- Group B: sand like, or most particles of size 40 μm$<d_p<$ 500 μm and density $1.4<\rho_s<4$ g/cm$^3$. These solids fluidize well with vigorous bubbling action. In this case, bubbles grow large as they rise in the fluidizing bed.
- Group D: spoutable, or large and/or dense particles. Deep beds of these solids are difficult to fluidize. They behave erratically, exhibiting large exploding bubbles, severe channelling or spouting behaviour if the gas distribution is uneven. Grain and pea drying, coffee bean roasting, coal gasification and ore roasting are such kind of fluidization systems. They are usually processed in a shallow bed or in the spouting mode.

Other attempts to describe fluidization regimes also include an assessment of pressure fluctuation, voidage and bubbling properties (Andreux et al., 2005). To date, no single method has been commonly accepted, but Geldart's regime classification (Geldart, 1986) remains the simplest and most acknowledged.

In order to understand and generalize the movement of solid particles during fluidization, different attempts have been made to visualize the fluidized bed. Sufficient understanding of the particulate segregation/mixing mechanism is quite important in designing gas-solid fluidization systems. The segregation characteristics depend on many factors, e.g. the density ratio between particles, size ratio of particles, shape of particles, fluidization gas velocity, distribution of fluidization gas and material packing ratio. To examine the effect of these factors on particle segregation, various approaches have been attempted, such as the direct observation of a two-dimensional bed, rapid shut

off method, radioactive isotope tracer study, and X-ray photography (Umekawa et al., 2005). Earlier attempts involved two-dimensional observations of a fluidized bed in a thin column, but it was soon found that this method is inadequate to represent fluidized bed because of the profound wall effect during fluidization. In more recent studies, both intrusive and non-intrusive methods have been used. Intrusive methods include probing, viscosity measurement and draw yield plate analysis. Non-intrusive methods are mostly tracer studies (Dechsiri et al., 2005). Despite the massive efforts to understand the fluidization system, generalized insight is limited. The main obstacle is that the characteristics of a fluidized bed behave and change erratically depending on the solid particles and fluidization velocity used. In order to have a complete generalization about the fluidization system, each experimental variable needs to be studied individually and extensively in a systematic manner.

Despite the lack of generalization on characterizing gas-solid fluidized beds, a few observations are agreed upon by most researchers in this area:

- A bed at minimum fluidizing conditions can be treated as a liquid of low or negligible viscosity. At higher velocities the excess gas goes through the bed as bubbles, which rise as in an ordinary liquid of low viscosity (Geldart, 1973).
- The level of segregation (settling of larger and denser particles to the bottom of the bed) increases with an increase in the width of the particle size distribution (Dahl and Hrenya, 2005).
- The shapes of bubbles are somewhat alike, close to spherical when small, flattened and distorted with a spherical cap-shape when large (Geldart, 1973).

- The voidage of a bed, not counting bubbles, remains close to $\varepsilon_{mf}$. At minimum fluidizing condition, the solids are relatively quiescent. At higher gas velocities, the rising bubbles cause the observed churning, mixing and axial transport of solids (Kunii and Levenspiel, 1991).
- The region just below the rising bubble is the wake region. The turbulence caused by this region results in solids being dragged up behind the bubble. A rising bubble drags a wake of particles up through the bed, shedding and leaking solids as it travels (Rowe and Partridge, 1965).
- Bed voidage increases with increasing fluidization gas velocity (Sidorenko and Rhodes, 2004).
- "Gulf streaming" is a model used to account for solids movement in the bed. Because of a non-uniform bubble distribution over the bed cross section, regions exist where, in addition to the wake material, bulk material (interstitial between the bubbles) is also dragged up with the bubble stream. This flow of bulk material can be considerably larger than the wake flow, causing a considerable faster downward bulk flow in the rest of the bed (Merry and Davidson, 1973).
- Dechsiri et al. (2005) proposed the behaviour of gulf streaming from extremely bad to ideal cross-sectional bubble distribution:
    a) Very bad bubble distribution leads to a highly localized region of high material (particle) activity and velocity. The bulk material flows rapidly upward in this region, and relatively slowly downward in the rest of the bed.

b) Better bubble distribution gives a larger region of slightly lower bubble activity. The upward flow of the bulk material in this region is larger in terms of volume but smaller in terms of velocity than in case a) above.

c) With ideal bubble distribution, where material is brought upward only in bubbles' wakes, the downward velocity in the bulk is low and uniform across the bed.

## 2.2 *Use of ADMFB for coal cleaning*

The ADMFB utilizes a gas-solid medium to form not only a pseudofluid, but also a stable and uniform air-solid suspension of a desired density, depending on the physical properties of the solid particles forming the bed. By introducing a coal feed into the separation medium, coal particles with high mineral matter content (rejects) possessing a higher density than that of the fluidized bed will sink. Coal particles with low mineral matter content (cleaned coal), possessing a lower density than that of the fluidized bed, will float. This results in a density-based particle separation of low mineral matter content coal particles and high mineral matter content rejects particles. Compared with a pneumatic-only system, the ADMFB separator provides a more accurate density-based particle stratification and hence an increased separation efficiency. For this reason, the ADMFB separator has demonstrated some degree of commercial success for cleaning coal coarser than 6 mm (Luo et al., 2003b).

A main anticipated reason why the ADMFB separator is unable to separate finer coal is that the rising bubbles encourage back-mixing of the rejects particles in the

fluidized bed (Luo et al., 2003b). To minimize the effect of back-mixing, researchers have tried to use finer-sized medium particles (Choung et al., 2006) and apply external energies such as an electric field (Kleijn van Willigen et al., 2005), mechanical vibration (Jin et al, 2005) or a magnetic field (Luo et al., 2003a) to destroy bubble formation and/or to stabilize the suspension during fluidization. Luo et al. (2003) reported high separation efficiency on coals as fine as 0.5 mm with the assistance of bed stabilization using a magnetic field during fluidization.

Due to the fact that the cost of equipment to monitor fluidized bed hydrodynamic is high, a limited number of studies to understand the actual mechanism of rejects being carried over from the bottom of the fluidized bed have been performed. The existing findings all support the fact that there is a narrow operating range between the maximum (where carry-over of rejects occurs) and the minimum fluidization gas velocity (where a stable suspension forms) where maximum separation efficiency is achieved (Jin et al., 2005; Oshitani et al., 2004; Choung et al., 2006).

The main objective of this study is to evaluate the effect of fluidization air velocity on ADMFB separation efficiency of an Alberta sub-bituminous coal. Compressed air is used as the fluidization gas in this study.

## 2.3 *Association of mercury with mineral matters in coal*

The majority of mercury in water, soil, sediments, plants and animals is in the form of inorganic mercury salts and organic forms of mercury, primarily methyl mercury (Goodarzi, 2004). In Canada, mercury releases are typically attributed to waste

incineration, coal combustion, base metal smelting and the chlor-alkali industry (Environment Canada, 2004). These activities have influenced the redistribution of mercury from geogonic sources into the air, water and topsoil.

The most common approach for removing mercury from coal-fired power plants is to capture the mercury vapour in the utility flue gas after combustion. Although this method has been effective at removing mercury in municipal waste incinerators, tests conducted to date on coal-fired boilers show that mercury removal from utility flue gas is much more difficult (Carey et al., 2000).

An option for controlling the release of toxic elements from coal into the atmosphere is to remove them before combustion. The degree to which a specific trace element can be reduced by coal cleaning depends on the mode of occurrence of that trace element, the method of cleaning employed and the way in which the cleaning process is operated. In addition to reducing the concentration of toxic elements, coal cleaning can improve overall boiler performance by increasing thermal efficiency. Also, coal cleaning changes ash loading and ash chemistry, improving the performance of particulate collection equipment (Akers and Dospoy, 1994).

While there are existing measurement techniques, such as isotope dilution cold-vapour inductively coupled plasma mass spectrometry, for high accuracy determination of the mercury concentration in bituminous and sub-bituminous coals (Long and Kelly, 2002), the distribution of mercury in the coal matrices (carbon-rich phase and/or mineral matters) remains unresolved.

Identifying mercury association in coal allows the development of the best removal strategies. If mercury is mainly associated with the mineral matters in coal, coal

cleaning would provide an economical and effective method for mercury removal. Mineral matters that contain mercury can be rejected from the as-mined coal before coal utilization, and thus, the difficulties associated with capturing mercury vapour from the flue gas can be avoided.

Upon successful concentration of cleaned coal and rejects particles by ADMFB separation, mercury analysis was employed to establish whether there is a correlation between mercury and ash-forming mineral matters.

# CHAPTER 3 MATERIALS AND EXPERIMENTAL SETUP

## 3.1 *Materials*

### 3.1.1 Media particles

The magnetite particles used as the fluidizing medium were purchased from Ward's Natural Science Establishment in Utah, USA. Silica sand used in this study was purchased from Sil Industrial Minerals, Canada.

### 3.1.2 Coal

Sub-bituminous coal samples were obtained from the Fording Mine near Genesee, Alberta, Canada. Two coal samples were received and labeled as Seam 1 and Seam 2. The coal samples were air dried at ambient conditions for 7 days. For ADMFB experiments, the dried coal samples were reduced in size using an Allis Chalmers jaw crusher (Milwaukee, USA). The crushed samples were classified into five size fractions: 22.6x1.00 mm, 22.6x5.66 mm, 5.66x3.36 mm, 3.36x1.00 mm and -1.00 mm.

## 3.2 *Experimental setup*

### 3.2.1 Process schematics

The experimental configuration was the same for both the 5-cm and the 20-cm diameter ADMFB devices. The ADMFB system used in this study is shown schematically in Figure 3-1.

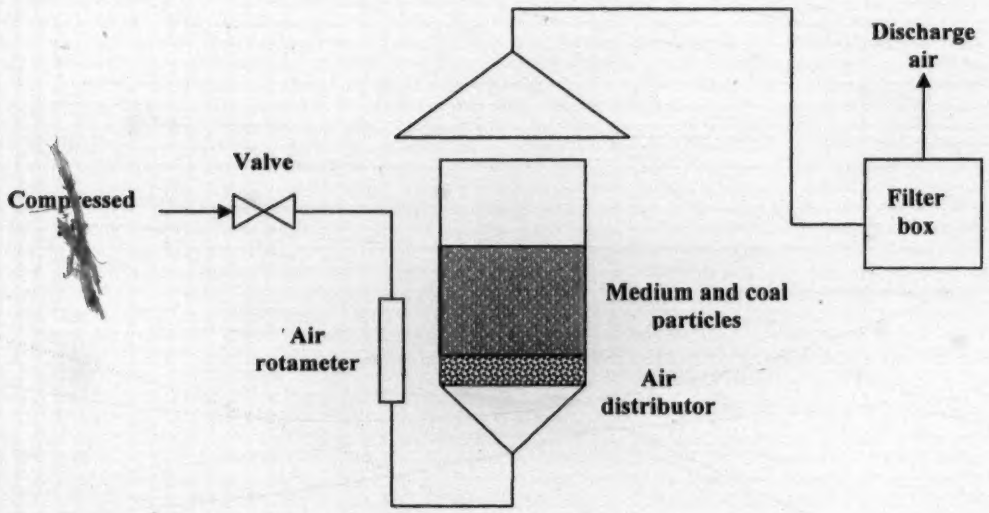


Figure 3-1. Process diagram of the air dense medium fluidized bed separator.

In the ADMFB experiments with the 5-cm diameter separator, a glass cylinder of 10 cm tall and 5 cm in diameter was attached to an air distributor. The air distributor was a porous glass plate with an average pore size of 40 μm and thickness of 1 cm. Medium particles were placed on the air distributor to a desired height, measured using a metric ruler. The precision of the metric ruler was 0.1 cm. The flow of compressed air was

controlled by a valve and measured by a rotameter from Cole Palmer. The precision of the rotameter was 0.1 cm/s. The compressed air pressure was kept at a constant level of 40 psig.

In the ADMFB experiment with the 20-cm diameter separator, a vertical Plexiglas cylinder of 40 cm tall and 20 cm in diameter was attached to an air distributor. The air distributor was a porous metallic plate with an average pore size of 40 μm and thickness of 0.3 cm, purchased from the Matt Corporation in Farmington, Illinois. Medium particles were placed on the air distributor to a desired height, measured using a metric ruler with a precision of 0.1 cm. The airflow rate through the air distributor was controlled by a valve and measured by a Blue-White rotameter. The precision of the rotameter was 0.1 cm/s. The compressed air pressure was kept at a constant level of 40 psig throughout the experiment. During fluidization, entrained particles in the exit air stream were collected using a Nederman's Filter Box (Helsingborg, Sweden). The filtered air was then discharged into the atmosphere.

### 3.2.2 Operation procedure

During an ADMFB experiment, medium particles were first placed into the column. The valve was fully opened, and the fluidization air velocity was adjusted by the rotameter. The compressed air entered and got evenly distributed by the porous plate at the bottom of the column.

When the minimum fluidization air velocity was reached, the medium particles became suspended by the uplifting air and formed an air-solids suspension in the column.

In this study, the fluidization air velocity refers to the superficial air velocity obtained by dividing the cross-sectional area of the column by the volumetric flow rate of the gas indicated on the rotameter. After the fluidized bed was developed, coal particles were manually and gently introduced to the surface of the fluidized bed and allowed to separate.

After 15 min of fluidization (unless indicated otherwise), the inlet air was rapidly shut off. Embedded with coal particles, the fluidized bed settled to a packed state. This is referred to as the rapid shut off method. The mixture of medium and coal particles was divided into four or more zones along the bed height manually by a metal scoop. In this study, the coal particles in each zone were isolated from the medium particles by a 1.00 mm opening sieve, although they could also be isolated by a magnetic separation method. After the medium particles were removed, the mass of each coal sample was recorded, and ash analysis was performed on each sample.

In the case of a pneumatic experiment, coal particles were placed into the column, and the coal particles were fluidized in a similar manner as in an ADMFB experiments. After 15 min of fluidization, the inlet air was rapidly shut off. The segregated coal particles were divided into four or more zones along the bed height manually by a metal scoop. The mass of coal sample collected in each zone was recorded, and ash analysis was performed on each sample.

The cumulative yield as a percentage of the feed sample weight (sum of samples collected from the top to the bottom of the fluidized bed) was calculated. The first data point was the ash and yield of the coal sample collected closest to the surface of the fluidized bed. The next data point was the cumulative yield and corresponding

cumulative ash content of the top two samples. Such cumulative calculation continued with the rest of the collected samples, and these data points were plotted accordingly.

Error bars were not established in the experimental results because coal samples of fixed cumulative yield or cumulative ash content could not be obtained from the experiments. As a result, only the experiments resulting in high separation efficiency for coal cleaning were repeated three times, and the data points generated were presented with the same symbol in the plots.

## 3.3 *Analyses*

### 3.3.1 Particle size distribution

U. S. standard brass sieves were purchased from Fisher Scientific Canada. Particle size distribution analyses were preformed on Ro-Tap test sieve shakers from W.S. Tyler. A minimum sample weight of 150 g was used for the analysis. The sizes of sieves selected depended on the top and bottom sizes of the sample. The sieving time was fixed at 15 min. After sieving, sample retained on each sieve was weighed. Particle size distribution was obtained by calculating the weight of sample retained in each size fraction as a percentage of total sample weight.

### 3.3.2 Density

This analysis was used to determine the density of the medium particles used for fluidization. Gay-Lussac specific gravity bottles (50 ml) were purchased from Fisher Scientific Canada. The bottles were thoroughly dried before each analysis. The weight of the empty bottle (with cap) was recorded, and an accurately weighed medium sample was placed into the bottle. Water of known density (with respect to water temperature) was then used to fill up the bottle. The bottle was connected to a vacuum pump to remove entrained air in the sample/water mixture. The bottle cap was inserted into the bottle to remove excess water. The exterior of the bottle was dried, and the total weight of the bottle and its content was recorded. The volume of the medium sample was calculated by subtracting the volume of the filled water from the bottle volume (50 ml). Finally, the specific gravity of the medium sample was calculated by dividing the weight of sample by the volume of sample.

### 3.3.3 Ashing

Ash analysis was performed with reference to the ASTM Method D 3174: Standard Practice for Proximate Analysis of Coal and Coke. After each ADMFB experiment, a Brinkmann-Retsch pulverizer was used to reduce particle size of coal sample to the size required for ash analysis. Purchased from Fisher Scientific Canada, 17-ml porcelain crucibles were dried before each analysis. A Denver Instrument analytical balance with 0.1 mg precision was used. The crucibles were weighed, and coal samples were placed into the crucibles. The crucibles with the containing coal samples

were dried in a desiccator for 4 hours, and their weights were recorded. The crucibles with the containing coal samples were placed into a Barstead-Thermolyne furnace at 750°C for 3 hours. The crucibles with the coal samples were removed and weighed as soon as they were cool in the desiccator. For calculation of ash content, please refer to the mentioned standard.

### 3.3.4 Float-sink test

For float-sink tests, ASTM Method D 4371-91: Standard Test Method of Determining the Washability Characteristics of Coal was followed. Liquid media in the *S.G.* range of 1.3 and 1.9 were prepared by mixing toluene, dibromomethane and/or tetrachloroethylene, purchased from Fisher Scientific Canada. The *S.G.* of the liquid medium was measured using a hydrometer purchased from Fisher Scientific. During the float-sink test, a coal sample was placed into the liquid medium of known *S.G.* and allowed to settle for 3 min. For coal samples coarser than 3.36 mm, a strainer with opening of 1.00 mm was used to remove the floating particles from the liquid medium. For coal samples finer than 3.36 mm, the floating particles were removed by pouring them along with the medium liquid onto a filter paper. The pouring was carried out slowly in order to not disturb the settled particles. The settled particles were then placed into the next liquid medium of higher *S.G.*. This procedure was continued with liquid mediums of progressively increasing *S.G.* until the majority of the coal particles floated. The weight of the particles floated in each liquid medium was recorded.

### 3.3.5 Mercury

For mercury content determination, a modified procedure (Crock, 2005) of ASTM Method 6414-01: Coal Digestion and Mercury Analysis was followed. A description of the modified procedure is attached as Appendix A. A Brinkmann-Retsch pulverizer was used to reduce the particle size of the coal sample to finer than 250 μm for analysis. A mercury analyzer (PSA 10.035 Millennium Merlin/Galahad System) from P S Analytical, England, was used. This analyzer employs cold vapour atomic fluorescence spectroscopy to determine mercury content. Mercury content analysis was conducted by Mr. Riley Beauchamp in the Department of Chemical and Materials Engineering at the University of Alberta.

# CHAPTER 4 ADMFB EXPERIMENTS WITH A 5-CM DIAMETER SEPARATOR

In the following two chapters, the results from the ADMFB separation of a sub-bituminous coal were presented and discussed. In this study, the potential of using an ADMFB to separate as-mined coal into cleaned coal (a concentrate of lower ash content) and rejects (higher ash content) was investigated. Effects of operating parameters on ADMFB separation efficiency were evaluated. The optimal operating condition was then used to estimate the applicability of this technology to coal cleaning. Since it has been established that this technology can effectively clean bituminous coal down to 6 mm (Luo et al., 2003b), focus of this study was on the ADMFB separation of sub-bituminous coal finer than 6 mm.

Columns of 5 cm and 20 cm diameters were used for the experiments. The experiments conducted using the 5-cm diameter ADMFB were to investigate the boundaries of the process parameters. Initial experiments performed using the 20-cm diameter ADMFB were to evaluate optimal process parameters. After optimal process parameters for the fluidization system were identified, characterizations of the fluidized bed and coal distribution were carried out by the rapid shut off method. Upon collection of cleaned coal and rejects samples, mercury analyses were performed to investigate the relationship between ash content and mercury content of the coal used in this study.

## 4.1 *Float-sink analysis of Seam 1 and Seam 2 coal*

After the as-mined coal was crushed and classified into various size fractions, float-sink tests were performed. The float-sink test results for coal in 22.6x5.66 mm, 5.66x3.36 mm, 3.36x1.00 mm and 1.00x0.420 mm size fractions are shown in Figures 4-1 for Seam 1 coal.

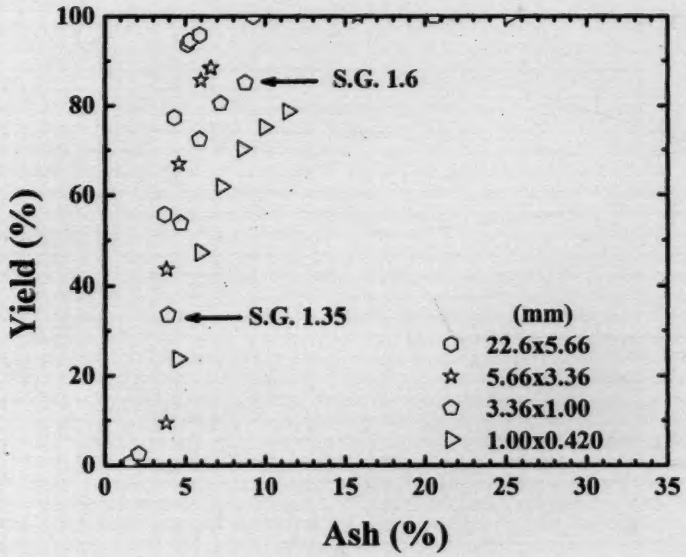


Figure 4-1. Float-sink analysis of crushed Seam 1 coal.

The ash contents of Seam 1 coal in size fractions of 22.6x5.66 mm, 5.66x3.36 mm, 3.36x1.00 mm and 1.00x0.420 mm were 9%, 16%, 21% and 28%, respectively. These results suggested that ash was highly liberated from the coal in 22.6x5.66 mm size fraction. It was anticipated that the liberated ash particles reported to the finer size fractions, led to an increase in ash content with decreasing particle size of coal. A sharp

decrease in yield was evident when ash content was further reduced to 6% for coal in the 22.6x5.66 mm and 5.66x3.36 mm size fractions. This observation indicated the amenability of coal in these size fractions to coal cleaning. The float-sink test results for coal in 22.6x5.66 mm, 5.66x3.36 mm, 3.36x1.00 mm and 1.00x0.420 mm size fractions are shown in Figure 4-2 for Seam 2 coal.

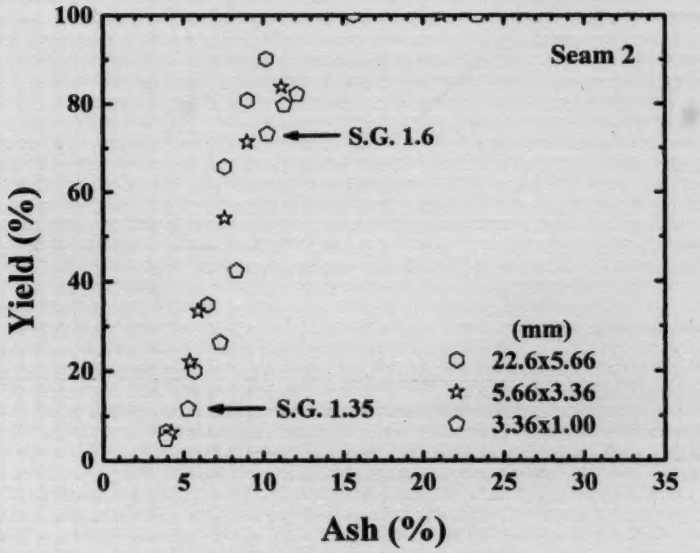


Figure 4-2. Float-sink analysis of crushed Seam 2 coal.

The ash contents of the Seam 2 coal in size fractions of 22.6x5.66 mm, 5.66x3.36 mm, 3.36x1.00 mm and 1.00x0.42 mm were 16%, 21%, 23% and 30%, respectively. The liberation of ash was evident, as shown by an increase in ash content with decreasing particle size of coal in Figure 4-2. The change in ash with yield was similar to the trend seen for the size fractions. It was obvious that Seam 1 coal would require less cleaning, since the overall ash contents of its size fractions were lower than those from Seam 2

coal. The float-sink results showed that cleaning of these two seams of coal was possible through density separation. This was shown by the increase in ash content of coal collected at increasing *S.G.* of medium within a narrow density range. The size-by-size ash contents for these two seams of coal are summarized in Table 4-1.

Table 4-1. Size-by-size ash content (%) of Seam 1 and Seam 2 coal.

| Size fraction (mm) | 22.6x5.66 | 5.66x3.36 | 3.36x1.00 | 1.00x0.42 |
|---|---|---|---|---|
| Seam 1 | 9 | 16 | 21 | 28 |
| Seam 2 | 16 | 21 | 23 | 30 |

## 4.2 *Fluidization classification of medium particles and coal*

Cleaning of coarse coal by ADMFB has been demonstrated by Chen et al. (2003) with a pilot plant that had a capacity of 50 t/h. Luo et al. (2003) reported satisfactory cleaning of bituminous coal as fine as 6 mm, but their study showed that this technology can not efficiently beneficiate coal finer than 6 mm. They have proposed two reasons: a) high viscosity and back-mixing of medium particles and b) unsuitable particle size ratio with medium particles being not sufficiently small compared to the coal particles. They further suggested that the back-mixing of medium particles was caused by the rising bubbles in the bubbling fluidized bed. According to the Geldart classification of fluidization, over 75% of the magnetite particles that Luo et al. (2003) used were Geldart B solids (see figure below) while the remainders were either Geldart A or Geldart C solids.

As reported by Geldart (1973), Geldart A solid formed fluidized bed with minimal bubbling, Geldart B solid formed bubbling fluidized bed and Geldart C solid was difficult to fluidize. Based on this characterization, it was not difficult to predict a poor separation of fine coal with the medium used by Luo et al. (2003). We intended to explore the desired fluidization of Geldart definition to extend the ADMFB method for fine coal cleaning.

As the compressed air was used in the current study, the density difference between the medium particles and gas was essentially the density of the medium particles since the density of the gas was negligible in comparison. In the experiments with the 5-cm diameter ADMFB, magnetite particles of decreasing size fractions were tested to evaluate the effect of medium particle size on coal cleaning. The magnetite particles used were represented by Region I in Figure 4-3.

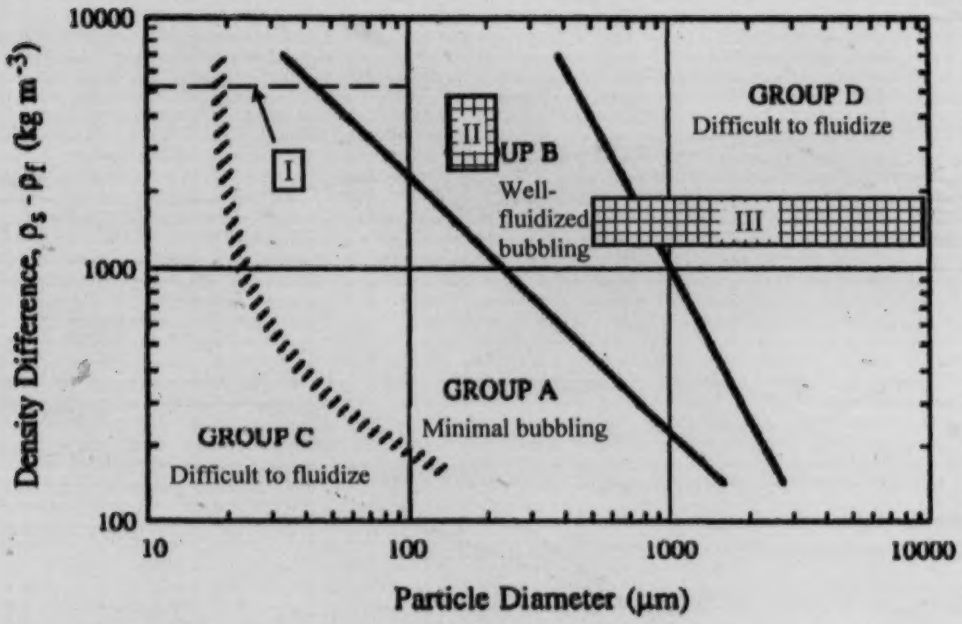


Figure 4-3. Fluidization classification diagram (Geldart, 1973).

For the magnetite particles represented by Region I, medium particles of smaller sizes were closer to the classification of Geldart C solid. The initial objective of this study was to minimize back-mixing of fine coal by using finer medium particles so that bubble formation could be suppressed.

In the experiments with the 20-cm diameter ADMFB, three media of different densities and sizes were used. These media were represented by Region II in Figure 4-3. It would be desirable to use different media with comparable sizes and/or densities to isolate the effect of medium particle size and the effect of medium particle density on ADMFB separation. Unfortunately, required quantity of such medium for the 20-cm diameter ADMFB experiments was not obtained during the course of this study.

From the float-sink analyses of crushed coal, it was found that the coal of lower ash content had a *S.G.* of about 1.4, while the coal of higher ash content had a *S.G.* of

about 1.8. Fluidization characteristics of the coal used in this study were indicated as Region III in Figure 4-3.

### 4.3 *Parameters investigation*

Before separation experiments were performed, the fluidization characteristics of the medium particles and coal particles in an ADMFB were investigated. A snap shot of the 5-cm diameter ADMFB separation device is shown in Figure 4-4.

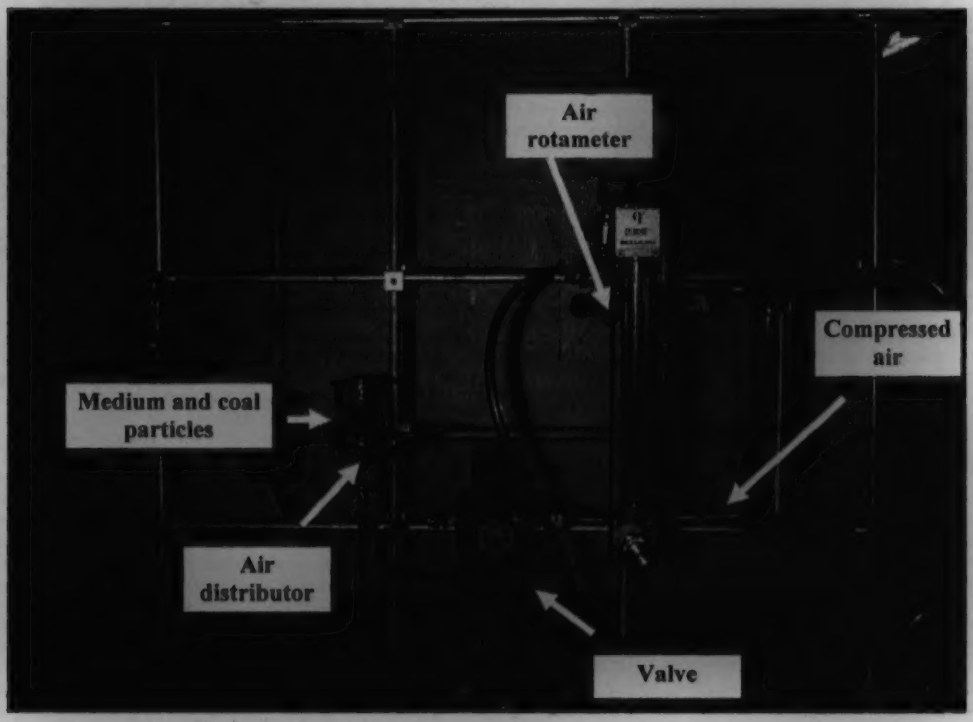


Figure 4-4. A photo of the 5-cm diameter ADMFB separation device.

All heights were measured from the air distributor located at the bottom of the column. As indicated in Figure 4-5, the packed bed height (a) was the height of the medium

particles before fluidization, and the fluidized base height (b) was the height of the interface that was relatively stable compared to the fluidized peak height during fluidization. The fluidized peak height (c) was the highest observed height of the rising bubbles when they emerged from the surface of the fluidized bed.

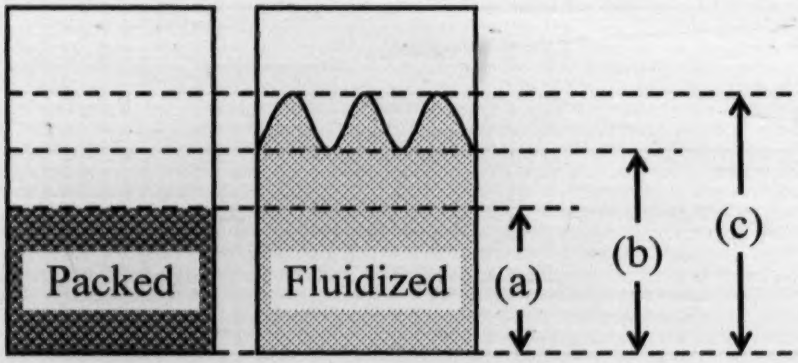


Figure 4-5. Fluidized bed height measurements: (a) Packed bed height, (b) Fluidized base height and (c) Fluidized peak height.

To demonstrate the differences between the packed bed height, fluidized base height and fluidized peak height, snapshots of the medium particles before and during fluidization are shown in Figure 4-6.

Figure 4-6. Snapshots of the packed bed (left) and fluidized bed (right): (a) Packed bed height, (b) Fluidized base height and (c) Fluidized peak height.

Snapshots of the fluidized bed using the 20-cm diameter separator (will be discussed in Chapter 5) were presented to visualize the difference between the packed and fluidized bed.

Magnetite particles with a density of 5.2 g/cm$^3$ and Seam 1 coal were used for the experiments with the 5-cm diameter ADMFB separator. Seam 1 coal was initially used because its degree of ash liberation was higher than that of Seam 2 coal. Separation of cleaned coal and rejects particles by ADMFB separation was expected to be easier with Seam 1 than Seam 2 coal.

### 4.3.1 Fluidized bed characterization

As an initial approach, the individual fluidization characteristics of magnetite particles and Seam 1 coal were examined. In this set of tests, the packed bed height was fixed at 1.0 cm (as indicated by (a) in these figures). The fluidization air velocity was calculated by dividing the cross sectional area of the column by the volumetric flow rate

of the compressed air. The bed was fluidized at a fluidization air velocity above which particles entrainment was observed. The changes in the fluidized peak bed height and fluidized base height were then measured with respect to decreasing fluidization air velocity. It should be noted that after the air was shut off, the bed height did not fall back to the original packed bed height because the medium particles were perforated after fluidization.

The interpretation of minimum fluidization was varied by researchers, and it was difficult to determine $u_{mf}$ without monitoring the pressure drop across the fluidized bed. Therefore, the minimum bubbling velocity ($u_{mb}$) was reported in this study because the state of minimum bubbling fluidization was more obvious to observe experimentally than minimum fluidization. In Figures 4-7 and 4-8, the effects of fluidization air velocity on bed expansion are shown for magnetite particles and Seam 1 coal.

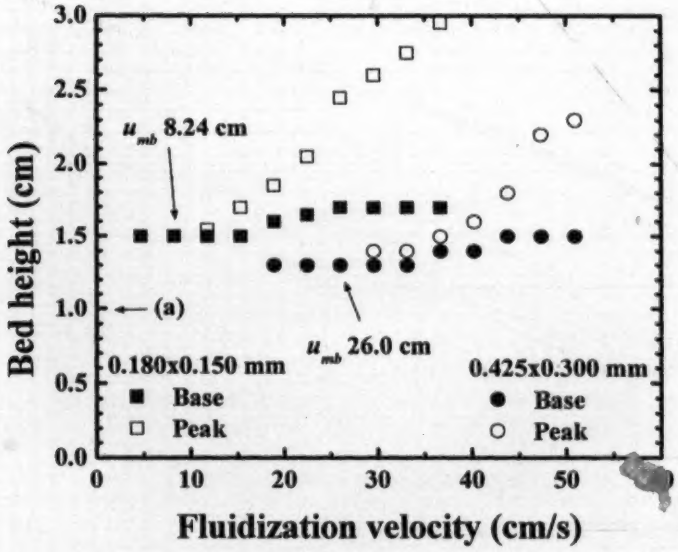


Figure 4-7. Effect of fluidization air velocity on bed height with a 5-cm diameter ADMFB separator and magnetite particles in two different size fractions.

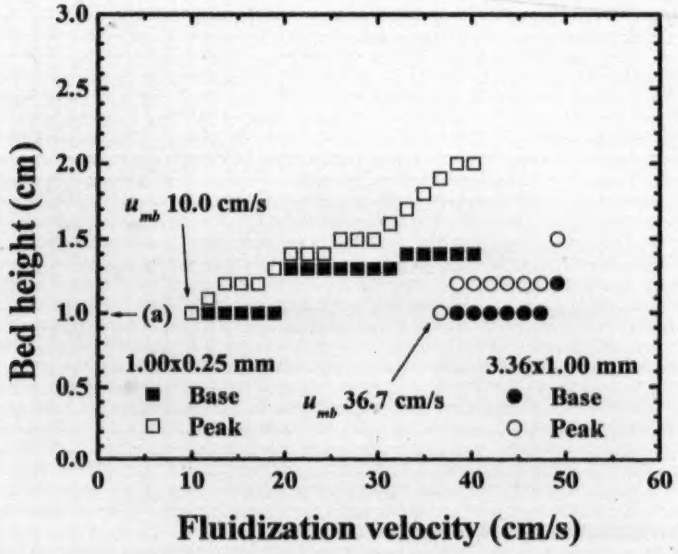


Figure 4-8. Effect of fluidization air velocity on bed height with a 5-cm diameter ADMFB separator and coal particles in two different size fractions.

The $u_{mb}$ of magnetite particles in 0.180x0.150 mm and 0.425x0.300 mm size fractions was determined to be 8.2 cm/s and 26.0 cm/s, respectively. The minimum bubbling height ($h_{mb}$) of the magnetite particles in 0.180x0.150 mm and 0.425x0.300 mm size fractions was measured to be 1.5 cm and 1.3 cm, respectively. It was observed that the magnetite particles in 0.180x0.150 mm size fraction expanded at a lower fluidization air velocity than the 0.425x0.300 mm size fraction. This was expected since the 0.425x0.300 mm magnetite particles lay closer to the Geldart D solid region (as shown in Figure 4-3) than the 0.180x0.150 mm magnetite particles. As a result, a higher fluidization air velocity was needed to fluidize coarser particles of the same density.

The $u_{mb}$ of coal in the 1.00x0.420 mm and 3.36x1.00 mm size fractions was 10.0 cm/s and 36.7 cm/s, respectively. The $h_{mb}$ of coal in the size fractions of 1.00x0.420 mm and 3.36x1.00 mm was 1.0 cm. The coal in the 1.00x0.420 mm size fraction was more readily fluidized than coal in the 3.36x1.00 mm size fraction. This was inferred from a sharper increase in fluidized peak height with increasing fluidization air velocity. Coal in the 1.00x0.420 mm size fraction was classified as a Geldart B solid while coal in 3.36x1.00 mm size fraction was a Geldart D solid. The observed fluidization characteristics agreed with the expectations of the Geldart classifications. A higher velocity was needed to fluidize the Geldart D solids than the Geldart B solids. Figures 4-7 and 4-8 showed that the $u_{mb}$ and $h_{mb}$ values were dependent on the size and density of the medium.

The initial approach in this study was to choose the finest possible medium particles to be fluidized so that the ADMFB separation could be operated at a minimal fluidization air velocity for more uniform and stable suspensions. The $u_{mb}$ of the

magnetite particles in 0.180x0.150 mm size fraction was 8.2 cm/s. Operation at this fluidization air velocity was relatively close to the $u_{mb}$ value of the finest coal (1.00x0.420 mm) studied. Based on such a consideration, further experiments were performed with magnetite particles finer than 0.150 mm to minimize the fluidization air velocity needed to form a stable fluidized bed. The aim was to choose a fluidization air velocity that was sufficiently low to properly fluidize the medium particles without fluidizing the fine-sized rejects particles. In this way, the feed coal particles could be separated into cleaned coal and rejects in a relatively quiescent environment.

Experimental observations on the fluidization characteristics of media tested with the 5-cm diameter ADMFB separator are summarized in Table 4-2:

Table 4-2. Physical properties and fluidization characteristics of media tested with 5-cm diameter ADMFB separator at 1.0 cm packed bed height.

| Medium | Size fraction (mm) | Density ($g/cm^3$) | Minimum bubbling velocity (cm/s) | Minimum bubbling height (cm) |
|---|---|---|---|---|
| Magnetite | 0.180x0.150 | 5.2 | 8.2 | 1.5 |
| Magnetite | 0.425x0.300 | 5.2 | 26.0 | 1.3 |
| Coal | 1.00x0.25 | 1.4-1.8* | 10.0 | 1.0 |
| Coal | 3.36x1.00 | 1.4-1.8* | 36.7 | 1.0 |

*The density range of interest.

The minimum bubbling height of coal was 1.0 cm for both size fractions studied. This observation showed that at minimum bubbling fluidization, the fluidized bed formed by coal alone did not expand from the initial packed bed height. In the case of the fluidized bed formed with magnetite particles, a bed expansion was observed at minimum bubbling

fluidization. It was anticipated that this bed expansion would provide extra space between particles for segregation.

### 4.3.2 Effect of medium particle size on ADMFB separation

Since fluidization air velocity and fluidized bed height were interdependent variables, it was impossible to examine the effects of these two variables individually during fluidization. For the 5-cm diameter ADMFB experiments with magnetite particles of different size fractions, the average fluidized bed height was the controlled variable. The effect of fluidization air velocity on ADMFB coal separation will be discussed in Chapter 5. The average fluidized bed height was the average value of the observed fluidized base height and fluidized peak height. The results in the previous section showed that the finer-sized magnetite particles exhibited a greater bed expansion than coarser particles. This observation was illustrated by the difference in the fluidized base height and fluidized peak height at the same fluidization air velocity (see Figure 4-7). To form a fluidized bed of the same average fluidized bed height, a higher fluidization air velocity was needed for coarser medium particles than for finer medium particles. Even though the average fluidized bed height was kept constant, the degree of fluidization was different for the medium of each size fraction. Such difference in the degrees of fluidization is shown in the schematics of Figure 4-9.

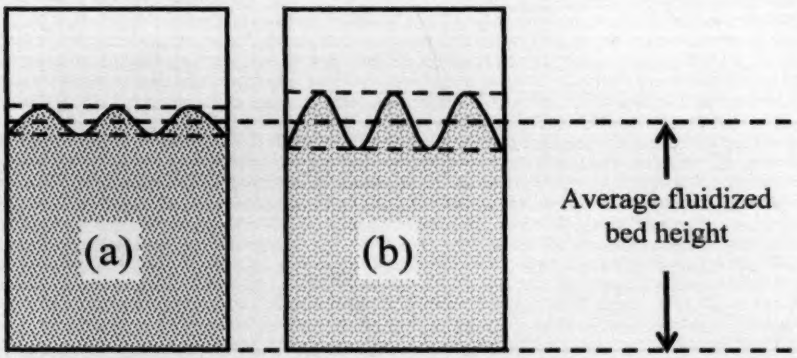


Figure 4-9. Schematic drawing of bed expansion during fluidization: a) Finer medium particles and b) Coarser medium particles.

The float-sink curve for the coal studied represented the ideal separation because it was truly a density-based separation, and the other physical properties of the coal (such as size and shape) would not contribute to the separation. It was important to distinguish this ideal separation from optimal separation discussed latter. Optimal separation only represented the maximum achievable separation with respect to a given fluidization system of medium and coal particles. The closer the ADMFB separation data was to the float-sink curve, the closer the ADMFB separation was to the ideal separation.

Magnetite particles in the -0.045 mm, 0.053x0.045 mm, 0.075x0.045 mm and 0.106 x0.045 mm size fractions were used in ADMFB for separation of coal in the 3.36x1.00 mm size fraction. The packed bed height was fixed at 2.0 cm. As shown in Figure 4-3, magnetite particles coarser than 0.045 mm belonged to Geldart A solid while magnetite particles in the other size fractions tested in the 5-cm diameter ADMFB experiments belonged to Geldart B solids. The separation results are shown in Figure 4-10.

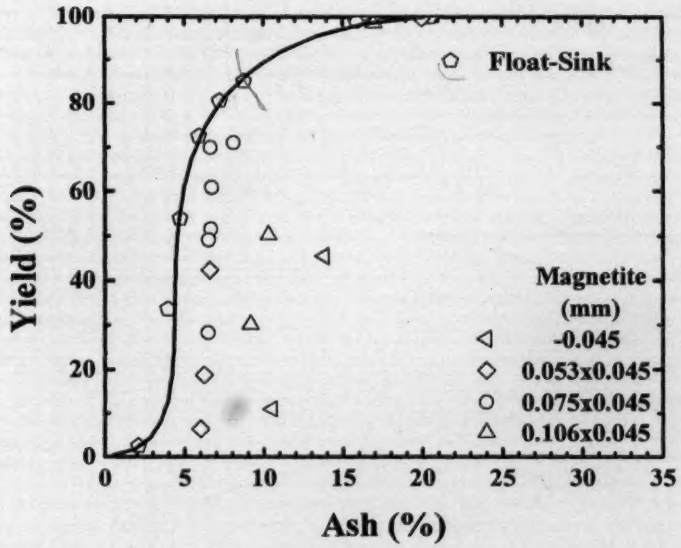


Figure 4-10. Effect of magnetite particle size on separation of coal in 3.36x1.00 mm size fraction.

To achieve the same average fluidized bed height of 2.2 cm during the experiments, a fluidization air velocity of 0.4 cm/s, 1.5 cm/s, 2.9 cm/s and 4.7 cm/s was used for the magnetite particles in -0.045 mm, 0.053x0.045 mm, 0.075x0.045 mm and 0.106x0.045 mm size fractions, respectively. The fluidization velocities tested were lower than the observed $u_{mb}$ of 36.7 cm/s required to fluidize coal in the 3.36x1.00 mm size fraction.

The separation results with the magnetite particles in 0.053x0.045 mm and 0.075x0.045 mm size fractions were closest to the float-sink curve, which represented the ideal separation. The results showed that the ADMFB bed formed by magnetite particles in 0.053x0.045 mm and 0.075x0.045 mm size fractions exhibited better separation than magnetite particles in the other size fractions. The ADMFB separations of coal using

magnetite particles in the 0.053x0.045 mm and 0.075x0.045 mm size fractions as media were similar. For the ADMFB formed by 0.075x0.045 mm magnetite particles, an ash reduction from 21% to 7% was achieved at 70% yield.

Compared to the separation obtained using the magnetite particles in 0.053x0.045 mm and 0.075x0.045 mm size fractions, the separation using the magnetite particles in 0.106x0.045 mm size fraction was found to be less efficient. The results suggested that magnetite particles in the 0.075x0.045 mm size fraction would allow the best separation with the fluidization system used. It was evident that the separation was not perfectly density-based since the experimental data points were still away from the float-sink curve.

The magnetite particles in -0.045 mm size fraction could not be fluidized at a fluidization air velocity below the $u_{mb}$ of the coal to be separated. The separation results produced by this bed were far from the float-sink curve. This observation indicated an inefficient separation. It was recognized that the magnetite particles in -0.045 mm size fraction belonged to Geldart A and/or Geldart C solids. The cohesiveness of these medium particles in this case would be so strong that the bed could not be properly fluidized at low fluidization air velocity. In these experiments, gas channelling, where the gas found fissures or other fixed passages through stationary medium particles, was observed. A stable fluidized bed could not be formed since these medium particles were not suspended by the incoming gas. For this reason, magnetite particles in the –0.045 mm size fraction were not tested further.

For the ADMFB formed by the magnetite particles in 0.053x0.045 mm and 0.075x0.045 mm size fractions, good separation for coal up to 5.66 mm was obtained.

Because a column of 5 cm diameter was used, representative ADMFB separation of coarser coal was not practical due to wall effects and was not tested. Testing results with coarser coal using a larger size separator are discussed in Chapter 5.

### 4.3.3 Effect of coal size (lower separation limit) on ADMFB separation

In an attempt to separate the coal in 1.00x0.42 mm size fraction, magnetite particles in the 0.053x0.045 mm, 0.075x0.045 mm and 0.106x0.045 mm size fractions were used to form ADMFB. In the previous section, a separation of cleaned coal and rejects was observed when medium particles in these size fractions were used. The fluidization air velocity used in the current tests was at 1.5 cm/s, 2.9 cm/s and 4.7 cm/s for magnetite particles in the 0.053x0.045 mm, 0.075x0.045 mm and 0.106 x0.045 mm size fractions, respectively. These fluidization air velocities were the same as in the previous separation experiments of coal in 3.36x1.00 mm size fraction,. The results are shown in Figure 4-11.

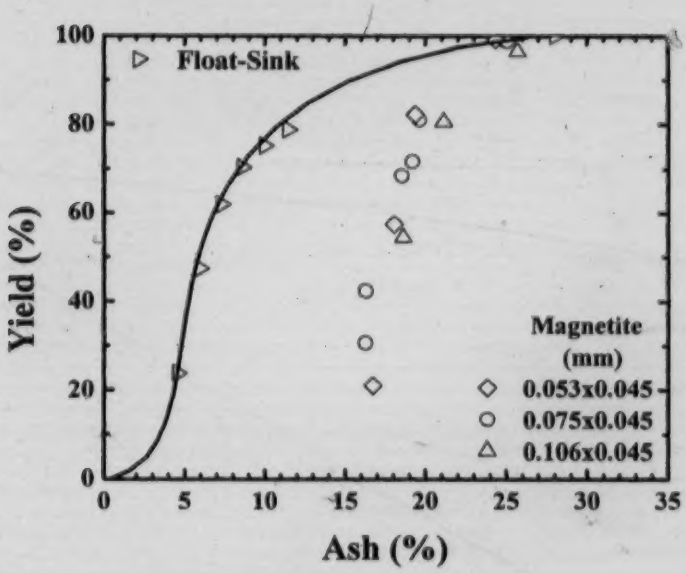


Figure 4-11. Effect of magnetite particle size on separation of coal in 1.00x0.42 mm size fraction.

The results in this figure showed that there was essentially no difference in separation efficiency for the three size fractions of magnetite particles used. This observation was illustrated by the trend the data points formed. This finding indicated that the ADMFB separation of coal in 1.00x0.42 mm size fraction was insensitive to the size of the medium particles used. Since the ADMFB formed by the magnetite particles in 0.075x0.045 mm size fraction showed good separation efficiency for 3.36x1.00 mm and coarser coal, the results in Figure 4-11 would suggest that 1.00 mm particles to be the lower size limit of coal suitable for ADMFB separation. At approximately 80% yield, the ideal ash reduction, as represented by the float-sink curve, would be from 28% to 11%. For the magnetite particles in 0.053x0.045 mm and 0.075x0.045 mm size fractions, an ash reduction from only 28% to 19% was obtained for the coal in 1.00x0.42 mm size

fraction. This reduction is low in contrast to that obtained for coal in 3.36x1.00 mm size fraction. It was not a surprise that the ADMFB could not achieve efficient separation for 1.00 mm and finer coal. Despite the lack of visual confirmation, it was speculated that the coal in 1.00x0.42 mm size fraction were circulating with the fluidizing medium particles. As a result, these coal particles could not be separated in terms of their density difference. According to the classification diagram in Figure 4-3, 1.00 mm coal marked the boundary line between Geldart B and Geldart D solids. The magnetite particles used were of Geldart B solids while coal particles finer than 1.00 mm were also of Geldart B solids. This observation suggested that medium particles used for the ADMFB and the coals to be separated must belong to different Geldart solids.

Since the reduction in magnetite particle size showed no improvement for separation of –1.00 mm coal, it was concluded that coal finer than this size was not suitable for ADMFB separation. The results also demonstrated that operation at a fluidization air velocity below the $u_{mb}$ of coal could not guarantee that the back-mixing of coal particles in the fluidized bed would not occur. It was evident that ADMFB separation efficiency decreased with decreasing particle size of coal.

### 4.3.4 Comparison of ADMFB and pneumatic separation

For the remainder of the study, attention was focused on the ADMFB separation of 3.36x1.00 mm and coarser coal due to poor efficiency of this method for finer coals. The separation of coal in 3.36x1.00 mm size fraction also represented the lowest possible separation efficiency by ADMFB separation. In Figure 4-12, the optimal separation

achieved for 3.36x1.00 mm coal using the ADMFB and pneumatic method were compared.

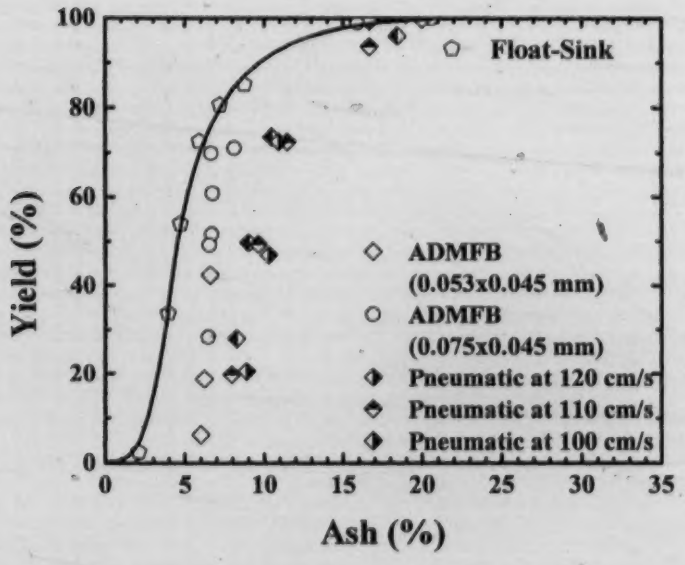


Figure 4-12. Comparison of ADMFB and pneumatic methods on separation of coal in 3.36x1.00 mm size fraction.

The fluidization air velocity used to form the ADMFB with the magnetite particles in 0.053x0.045 mm and 0.075x0.045 mm size fractions was 1.5 cm/s and 2.9 cm/s, respectively. For the pneumatic experiments, the coal in 3.36x1.00 mm size fraction was used to form a 2.2-cm packed bed height and fluidized without an additional medium. From the results in Figure 4-8, the observed $u_{mb}$ of the coal in 3.36x1.00 mm size fraction was determined to be 36.7 cm/s. As shown in Figure 4-12, much higher fluidization air velocities at 120, 110 and 100 cm/s were needed to achieve optimal pneumatic

separation. A higher required fluidization air velocity was anticipated to achieve optimal pneumatic separation for two reasons: a) the packed bed used in the pneumatic experiment was higher (packed bed height of 2.2 cm) and b) the coal bed did not expand at minimum bubbling condition. As a result, the coal particles needed to become more fluidized in order to have space for the rejects coal particles to segregate to the bottom.

As shown in Figure 4-12, the data points from the ADMFB tests were much closer to the float-sink curve than those from pneumatic tests. At about 70% yield for example, the ADMFB separation led to an ash reduction from 21% to 7%, while the pneumatic method reduced the ash content from 21% to 11%. It was evident that the ADMFB separation had a higher efficiency than the pneumatic separation for coal cleaning.

A higher fluidization air velocity was needed to achieve optimal separation in the pneumatic method than in the ADMFB method. This was expected since coal particles in this size fraction belonged to Geldart D solids, which were difficult to fluidize. It was proposed that the additional suspension provided by the ADMFB could be the main factor that contributed to the superior separation by of this method than by the pneumatic method.

## 4.4 *Summary*

Float-sink analyses were performed on the coal seams studied. The results showed that a density-based separation process was suitable for cleaning these coals. ADMFB experiments were performed with a 5-cm diameter separator. The fluidization

characteristics of magnetite particles and coal particles in various size fractions were studied. It was observed that the minimum bubbling velocity increased with increasing particle size of medium. Upon minimum bubbling fluidization, the fluidized bed formed by the coal particles did not expand from the initial packed bed height. The fluidization characteristics of the media agreed well with Geldart's fluidization classification diagram.

The ADMFB experiments with the 5-cm diameter separator showed that ADMFB separation had potential for coal cleaning. The results suggested that the magnetite particles (5.2 $g/cm^3$) in 0.075x0.045 mm size fraction would allow the best separation with the fluidization system used. With reference to Geldart's classification, the experimental results suggested that Geldart B medium would be optimal for ADMFB separation. It was also concluded that coal finer than 1.00 mm was not suitable to be effectively separated by ADMFB.

Under the optimal separation conditions, the separation by the ADMFB was found to be more effective than by the pneumatic method. A much higher fluidization air velocity was needed to achieve optimal separation by pneumatic method than by ADMFB method. It was anticipated that the pneumatic separation needed a higher fluidization air velocity to create voidage for particles to segregate.

# CHAPTER 5 ADMFB EXPERIMENTS WITH A 20-CM DIAMETER SEPARATOR – PARAMETERS OPTIMIZATION

From this section and onward, all discussions pertained to the ADMFB experiments conducted with a 20-cm diameter column. Since Seam 2 coal had higher ash content than Seam 1 coal, it had a greater need for coal cleaning to improve coal burning. For this reason, ADMFB separation of Seam 2 coal was investigated. Unless otherwise stated, ADMFB separations were performed with the coal particles in 22.6x1.00 mm size fraction without further size classification. After the separation, the collected coal samples in 22.6x1.00 mm size fraction were classified into three size fractions. The respective ash contents of the samples were determined. ADMFB separation efficiency was evaluated for coal in three size fractions: 22.6x5.66 mm, 5.66x3.36 mm and 3.36x1.00 mm. The coal samples in these size fractions belonged to Geldart D solids.

From the ADMFB experiments using the 5-cm diameter column, it was observed that Geldart B magnetite particles formed an effective ADMFB to clean coal of Geldart D characteristics. Three types of medium particles of different densities and size distributions were tested. These media particles exhibited of Geldart B particle characteristics. The particle size distributions of the media tested are shown in Figure 5-1.

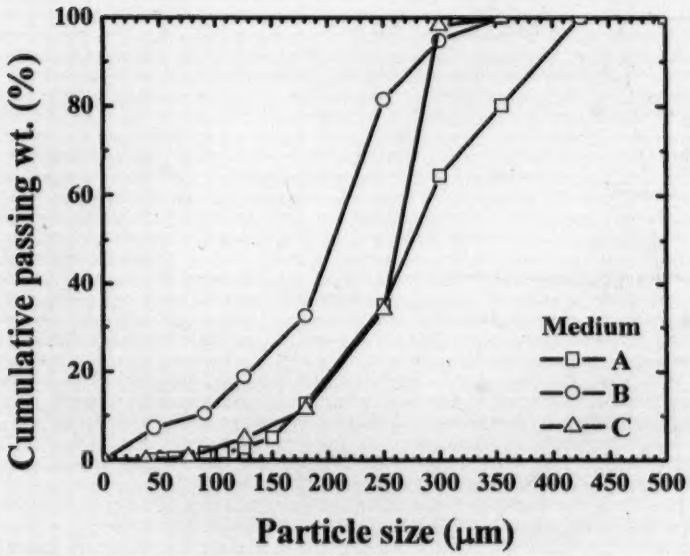


Figure 5-1. Particle size distributions of media.

Medium A had the largest median particle size while Medium B had the smallest median particle size. The particle size distribution of Medium C was intermediate between Medium A and Medium B. Medium C had the narrowest size distribution of the media tested. The density and median particle size of each medium are reported in Table 5-1.

Table 5-1. Physical properties of media used in a 20-cm diameter ADMFB separator.

| Medium | Material | Density ($g/cm^3$) | Median particle size* (μm) | $u_{mf}$** (cm/s) |
|---|---|---|---|---|
| A | Magnetite | 4.8 | 278 | 9.4 |
| B | Magnetite | 3.3 | 208 | 5.5 |
| C | Sand | 2.7 | 262 | 7.8 |

*The particle diameter at which the cumulative passing weight of particles is 50% in a size distribution curve.

**Calculated values, please refer to Appendix B for details on sample calculation.

Medium particles with controlled size and density would be highly desired to investigate the effect of physical properties of medium particles on separation efficiency. Unfortunately, sufficient quantities of such medium particles were not obtained, and only the media mentioned above were used.

## 5.1 *Fluidized bed characterization*

In Figures 5-2, 5-3 and 5-4, the effects of fluidization air velocity on bed expansion are shown for the three media used.

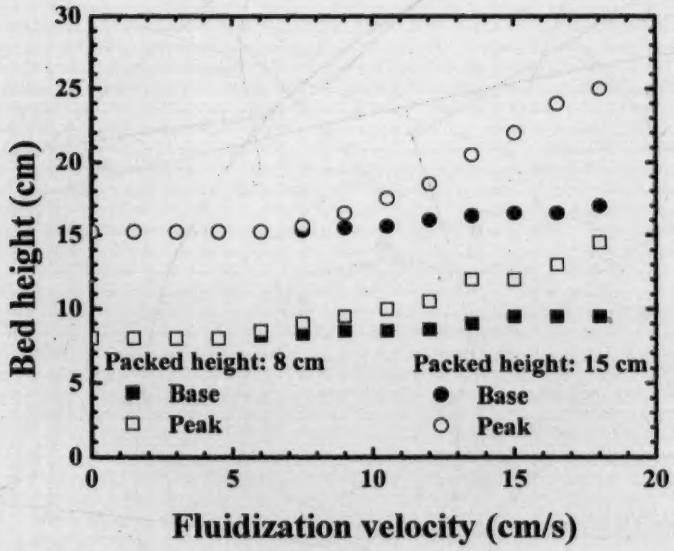


Figure 5-2. Effect of fluidization air velocity on bed height of Medium A in a 20-cm diameter ADMFB separator.

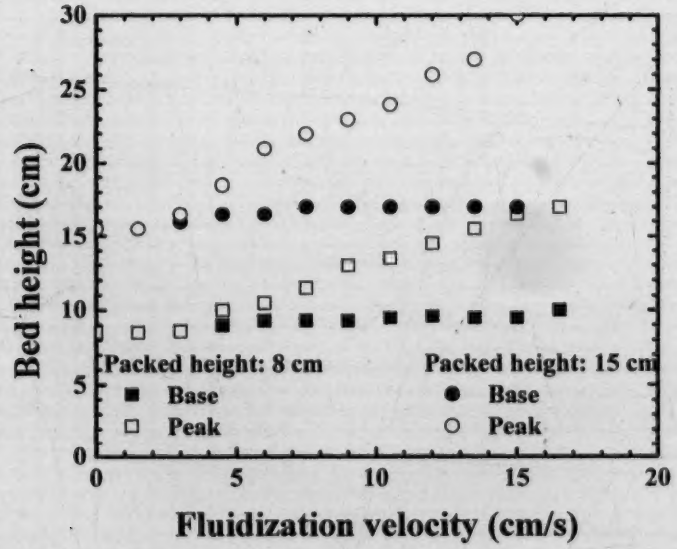


Figure 5-3. Effect of fluidization air velocity on bed height of Medium B in a 20-cm diameter ADMFB separator.

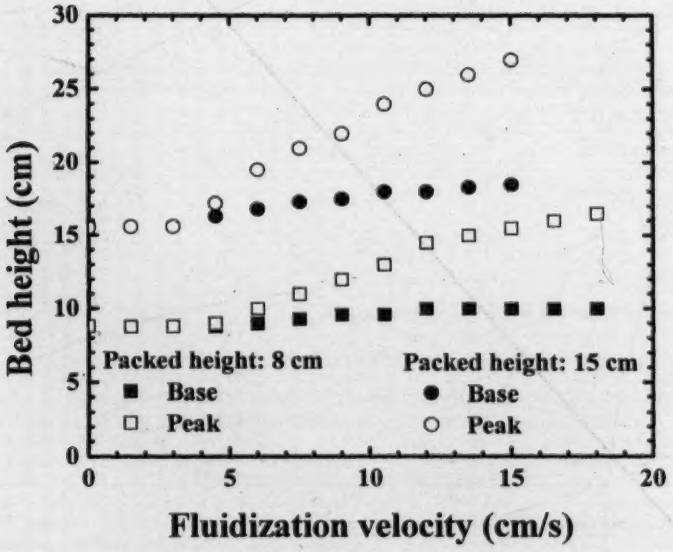


Figure 5-4. Effect of fluidization air velocity on bed height of Medium C in a 20-cm diameter ADMFB separator.

Packed bed heights of 8 cm and 15 cm were studied. The fluidized bed height was measured with decreasing fluidization air velocity in order to avoid the bed height from falling to the original packed bed height. No obvious difference was observed in terms of $h_{mb}$ values determined for the media studied. The $u_{mb}$ of Medium A was the highest amongst the media studied. In comparison, the fluidization characteristics of Media B and C were similar. The $u_{mb}$ and $h_{mb}$ of the medium particles are summarized in Table 5-2.

Table 5-2. Fluidization characteristics of media in a 20-cm diameter ADMFB separator at packed bed heights of 8 cm and 15 cm.

| Packed bed height (cm) | 8 | | 15 | |
|---|---|---|---|---|
| Medium | $u_{mb}$ (cm/s) | $h_{mb}$ (cm) | $u_{mb}$ (cm/s) | $h_{mb}$ (cm) |
| A | 4.5 | 8.0 | 6.0 | 15.2 |
| B | 3.0 | 8.5 | 3.0 | 15.5 |
| C | 3.0 | 8.8 | 3.0 | 15.6 |

## 5.2 *Effect of fluidization air velocity on ADMFB separation*

It was observed with the 5-cm diameter ADMFB separator that the characteristics of the fluidized bed had a direct effect on coal separation. The ADMFB separation efficiency deteriorated with decreasing particle size of coal. In the 5-cm diameter ADMFB experiments, the controlled parameter was the average fluidized bed height. For Seam 1 coal in the 3.36x1.00 mm size fraction, fluidized bed formed with the magnetite particles in 0.075x0.045 mm size fraction was found to provide optimal separation for the fluidization system tested. Most findings suggested the existence of a state where the vertical transport of the medium particles was minimized by adjustment of the fluidization velocity. If the vertical transport of medium particles was minimized, coal particles would be more effectively separated based on density differences, as disturbance from separation medium would be minimized.

In this section, the effect of fluidization air velocity on coal separation was evaluated for the case where the average fluidized bed height was not fixed. In these ADMFB experiments with a 20-cm diameter column, crushed coal particles of 22.6x1.00

mm were tested. The amount of coal tested was approximately 300 g for each experiment. The size distribution of the coal particles tested is given in Table 5-3.

Table 5-3. Size distribution of coal particles used for ADMFB experiment with a 20-cm diameter ADMFB separator.

| Size fraction (mm) | 22.6x1.00 | 22.6x5.66 | 5.66x3.36 | 3.36x1.00 |
|---|---|---|---|---|
| Weight (%) | 100 | 55 | 20 | 25 |

In this set of tests, the packed bed height formed by the medium particles was kept at 15 cm. The extents of bed expansion relative to the fluidization air velocity were shown in Figures 5-2, 5-3 and 5-4 for the media studied. After separation, the collected coal sample from each separation zone (along the bed height) was classified in to three size fractions: 22.6x5.66 mm, 5.66x3.36 mm and 3.36x1.00 mm. The size-by-size yield and corresponding ash content were determined. The fluidization air velocity was increased above $u_{mb}$ until an optimal achievable separation was obtained. The state of optimal achievable separation was determined by the proximity of the ADMFB separation results to the corresponding float-sink curve.

The effects of fluidization air velocity on separation efficiency of the coal in 22.6x1.00 mm with respect to the 22.6x5.66 mm, 5.66x3.36mm and 3.36x1.00 mm size fractions are shown in Figures 5-5, 5-6 and 5-7, respectively. In these tests, the fluidized bed was formed by Medium B.

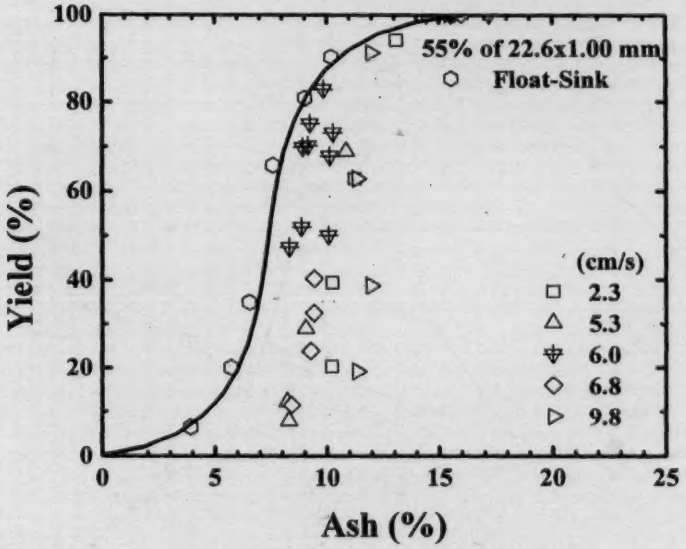


Figure 5-5. Effect of fluidization air velocity on ADMFB separation of coal in 22.6x5.66 mm size fraction with Medium B as separation medium.

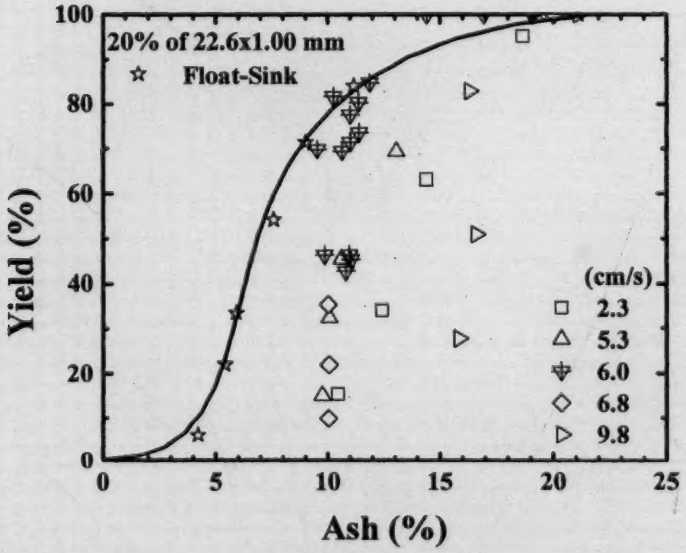


Figure 5-6. Effect of fluidization air velocity on ADMFB separation of coal in 5.66x3.36 mm size fraction with Medium B as separation medium.

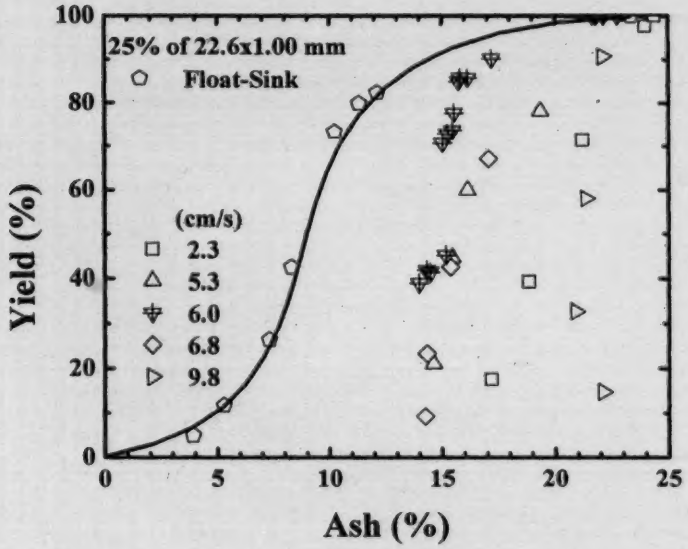


Figure 5-7. Effect of fluidization air velocity on ADMFB separation of coal in 3.36x1.00 mm size fraction with Medium B as separation medium.

The effect of fluidization air velocity on ADMFB separation efficiency was the most significant for the coal in 3.36x1.00 mm size fraction. For the coal in this size fraction, the optimal separation was obtained with the fluidization air velocity between 5.3 cm/s and 6.8 cm/s. This observation was shown by the closeness of these ADMFB separation results to the float-sink curve in Figure 5-7. Interestingly, a similar optimal fluidization air velocity range was also required for coal in the other two size fractions, as shown in Figures 5-5 and 5-6.

The optimal separation results for the 22.6x5.66 mm coal was close to the corresponding float-sink curve, while the optimal separation results for the 3.36x1.00 mm coal was relatively far away from its corresponding float-sink curve. At the optimal ADMFB separation condition, it was evident that the separation efficiency deteriorated

with decreasing particle size of feed coals. This observation was shown by the increase in the gap between the ADMFB separation results and the float-sink curves with decreasing particle size of feed coals.

In Figure 5-7, the lowest fluidization air velocity of the tests was set at 2.3 cm/s, which was close to the $u_{mb}$ of Medium B. It was evident that the ADMFB separation operated at this velocity was poor, as shown by a large gap between the ADMFB separation result and the float-sink curve. As the fluidization air velocity increased, the separation results shifted closer to the float-sink curve. This observation indicated that the ADMFB separation approached closer to the ideal separation for the coal in this size fraction.

As the fluidization air velocity increased beyond the optimal range, the ADMFB separation deteriorated. The results obtained with fluidization air velocities at 8.3 cm/s and 9.8 cm/s moved further away from the float-sink curve. At a fluidization air velocity of 9.8 cm/s with the 3.36x1.00 mm coal, it was observed that the ADMFB separation result deteriorated to an almost vertical trend. This finding indicated that the coal samples collected along the heights of the fluidized bed had the same ash content as the initial feed, and no beneficiation of coal occurred. A possible explanation for this observation was that such a high fluidization air velocity created too much back-mixing of particles (both medium and coal) for coal particles to segregate. As a result, the coal particles were circulating with the medium instead of segregating by density difference.

The results obtained so far agreed with the speculation that there existed an optimal fluidization air velocity for ADMFB separation. Increasing fluidization air velocity beyond the optimal range would deteriorate the separation. It was noted that the

optimal velocity was applicable for all the size fractions studied. This observation suggested that the ADMFB separation depended mainly on the quality of the fluidized bed. However, it remained to be established which characteristics of the fluidized bed would be the most appropriate to describe the quality of the bed for coal separation.

Despite the fact that optimal fluidization air velocity was independent of coal size, it was evident that the fluidization air velocity had a more profound effect on ADMFB separation of the coal in 3.36x1.00 mm size fraction. The coal in this size fraction was close to the established lower limit of coal size suitable for ADMFB separation. The results of ADMFB separations using the other two media for the coal in 3.36x1.00 mm size fraction are shown in the following figures. In Figure 5-8, Medium A was used to form the fluidized bed.

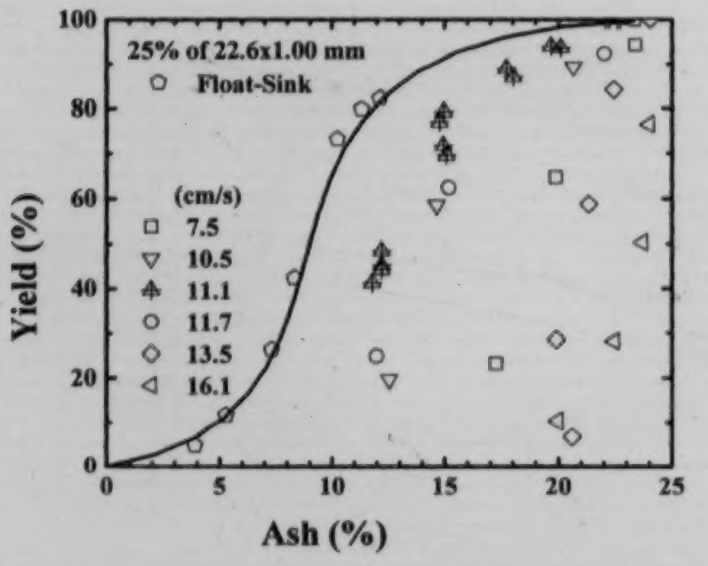


Figure 5-8. Effect of fluidization air velocity on ADMFB separation of coal in 3.36x1.00 mm size fraction with Medium A as separation medium.

Compared with Medium B (3.3 g/cm$^3$), the optimal fluidization air velocity of the denser Medium A (4.8 g/cm$^3$) was determined to be between 11.1 cm/s and 11.7 cm/s. This optimal fluidization air velocity range also applied to the coarser size coal when the same medium was used, as already discussed in Figures 5-5, 5-6 and 5-7. The fluidization velocities tested outside this range resulted in an ineffective separation. This observation was shown by the square, diamond and left-triangle symbols being far away from the ideal separation in Figure 5-8. An air fluidization velocity of 7.5 cm/s was slightly higher than the observed $u_{mb}$ of 6.0 cm/s and only 3.6 cm/s below the lower optimal fluidization air velocity. Operating at this fluidization air velocity only yielded an ash reduction from 23% to 20% at 65% yield. The fluidization air velocity at 11.7 cm/s represented the upper limit of the optimal fluidization air velocity range with Medium A. A satisfactory ash reduction from 23% to 15% at 63% yield was obtained. Increasing the fluidization air velocity to 13.5 cm/s, which was 1.5 cm/s above the upper limit of optimal fluidization air velocity, only resulted in an ash reduction only from 23% to 21% at 59% yield. This low level of ash reduction indicated that the ADMFB at this velocity was unable to form an effective fluidized bed to separate coal.

The results obtained using Medium C with the coal in 3.36x1.00 mm size fraction are shown in Figure 5-9.

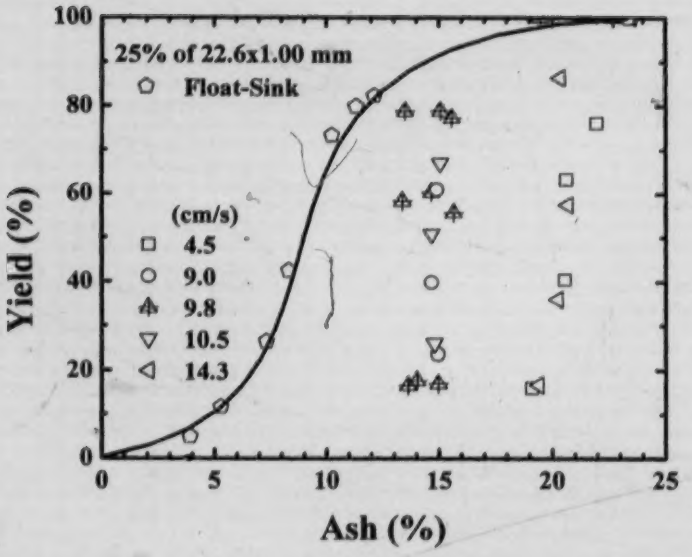


Figure 5-9. Effect of fluidization air velocity on ADMFB separation of coal in 3.36x1.00 mm size fraction with Medium C as separation medium.

Medium C had the lowest density (2.7 g/cm$^3$) among the media examined, and the optimal fluidization air velocity range was determined to be between 9.0 cm/s and 11.5 cm/s. The trend in this figure also suggested a narrow fluidization air velocity range for optimal separation. Outside this narrow range, a sharp decrease in separation efficiency was observed. To illustrate this observation, the amount of ash reduction at various fluidization air velocities was compared at a given yield of about 60%. The lowest fluidization air velocity tested was 4.5 cm/s, and the highest fluidization air velocity tested was 14.3 cm/s. At 4.5 cm/s, an ash reduction from 23% to 21% was obtained at 63% yield, while at 14.3 cm/s, an ash reduction from 23% to 21% was obtained at 58% yield. These fluidization air velocities resulted in an inefficient coal separation. At the

optimal fluidization air velocity of 9.0 cm/s, an effective ash reduction from 23% to 15% was obtained at a 61% yield.

From Figure 5-9, it was interesting to note that the results obtained at fluidization air velocities of 4.5 cm/s and 14.3 cm/s followed the same trend. During the ADMFB separation, it was observed that the bed fluidized at 4.5 cm/s was unable to support the weight of the coal because bed channelling (where gas bypassed through medium particles without fluidization) occurred upon coal addition. Under such a condition, the coal could not be stratified on a density basis because the fluidized bed was unable to provide a stable medium suspension for coal separation. The results clearly demonstrated that for coal separation, the fluidization air velocity should be operated above the corresponding $u_{mb}$. The bed fluidized at a fluidization air velocity of 14.3 cm/s did not collapse upon coal addition, but coal was found randomly distributed throughout the bed without any noticeable density-based stratification.

The above results showed that operation at a fluidization air velocity close to the corresponding $u_{mb}$ would result in a low separation efficiency because the fluidized bed could not support the weight of the coal added. Our study established that operation at an optimal velocity was required to create a fluidized bed that could support the additional weight of coal while not fluidizing fine coal along with the medium particles. A fluidized bed operated at a fluidization air velocity outside of the optimal range would result in low coal separation efficiency. Dechsiri et al. (2005) reported that under ideal bubble distribution condition, the downward velocity of the medium particles was low and uniform across the bed. The optimal fluidization air velocity found for each type of medium in this study could represent the state of the fluidized bed where the air (bubble)

distribution was ideal for optimal separation. Under this condition, back-mixing of medium particles was minimized.

An optimal fluidization air velocity range was found for each medium used in this study. Since the optimal fluidization air velocity was higher than $u_{mb}$, it was evident that the presence of bubbles was needed to achieve optimal ADMFB separation. The optimal fluidization air velocity and optimal fluidized bed height for each type of medium tested are summarized in Tables 5-4 and 5-5, respectively.

Table 5-4. Optimal fluidization air velocity for ADMFB separation in a 20-cm diameter separator with medium particles at a packed bed height of 15 cm.

| Medium | $u_{mb}$ (cm/s) | $u_{optimal}$ (cm/s) | $u_{optimal}/u_{mb}$ |
|---|---|---|---|
| A | 6.0 | 11.3 | 1.9 |
| B | 1.5 | 6.8 | 4.5 |
| C | 3.0 | 9.8 | 3.3 |

Table 5-5. Optimal fluidized bed height for ADMFB separation in a 20-cm diameter separator with medium particles at a packed bed height of 15 cm.

| Medium | $h_{mb}$ (cm) | $h_{optimal}$ (cm) | $h_{optimal}/h_{mb}$ | $h_{peak}$-$h_{base}$ (cm) |
|---|---|---|---|---|
| A | 15.2 | 15.8 | 1.0 | 2.0 |
| B | 15.5 | 16.8 | 1.1 | 4.5 |
| C | 15.6 | 17.8 | 1.1 | 5.0 |

The $u_{optimal}/u_{mb}$ was 1.9, 4.5 and 3.3 for Medium A, Medium B and Medium C, respectively. The $h_{optimal}/h_{mb}$ for Medium A, Medium B and Medium C was found to be 1.0, 1.1 and 1.1, respectively. For the three Geldart B media used, no obvious correlation

could be derived to link the minimum bubbling velocity to the fluidization air velocity for optimal separation. Compared with the calculated values of $u_{mf}$ reported in Table 5-1, there was no clear correlation between the minimum fluidization air velocity and the fluidization air velocity at optimal separation for each medium tested. The fluidized peak and base heights were considered, and there was also no obvious correlation that could be derived.

Using the optimal fluidization air velocity as determined above, the same experiment was repeated three times with each medium. During the repeat experiments, coal samples were collected at similar zones along the bed height. The results obtained were shown by the crossed symbols in Figures 5-5, 5-6, 5-7, 5-8 and 5-9. These figures showed that the repeatability of the laboratory ADMFB separation was acceptable. The change in ash reduction observed with increasing fluidization air velocity was considered likely to be a real effect rather than an experimental artifact.

Since optimal ADMFB separation could only be achieved over a narrow fluidization air velocity range, it was evident that the density of the fluidized bed was not adjustable by changing the fluidization air velocity. The separation results obtained using ADMFB strongly suggested that increasing fluidization air velocity beyond the optimal range would disrupt the density-based segregation of coal particles. A fluidization velocity higher than the optimal fluidization air velocity resulted in only a marginal ash reduction. As a result, the coal particles collected in all zones along the bed height showed ash contents similar to that of the feed. In a density-based separation, the ash content of the cleaned coal would decrease with decreasing separation density. In an ADMFB separation, increasing fluidization air velocity disturbed the segregation of the

coal particles. This increase in fluidization air velocity resulted in an increase of the ash content of the cleaned coal particles. The experimental results suggested that the apparent density of the fluidized bed was fixed within an extremely narrow range. This separation density was determined by the physical properties of the medium particles.

Since it was speculated that back-mixing of the fine coal was due to rising air bubbles, it was of interest to monitor the behaviour of the bubbles during fluidization. Unfortunately, suitable equipment was unavailable. The information regarding this topic in literature was rather limited and largely specific to particular fluidization systems.

### 5.3 *Estimate of medium particle size during optimal fluidization*

The size distribution of medium particles during fluidization at the optimal fluidization air velocity was examined in this section. Even though optimal separation efficiency was achieved by fluidization air velocity optimization, the respective size distribution of the medium particles in each zone along the bed height was largely unknown. To examine this behaviour, the inlet air was rapidly shut off during fluidization at an optimal fluidization air velocity, and the medium particles were collected from different zones along the bed height. Sieve analysis was used to determine the particle size distribution of medium particles collected in each zone. Since the medium particles collapsed immediately after the air was shut off, the size distribution of the medium particles analyzed using the collected particles in each zone should be representative of that zone during the fluidized state.

The median size of particles, at which the cumulative passing weight of particles was 50% on a size distribution curve, was determined. In Figures 5-10, 5-11 and 5-12, the median sizes of the particles collected at various static bed heights after fluidization are shown for Medium A, Medium B and Medium C, respectively. The overall median particle sizes of the media were indicated as the vertical lines in these figures.

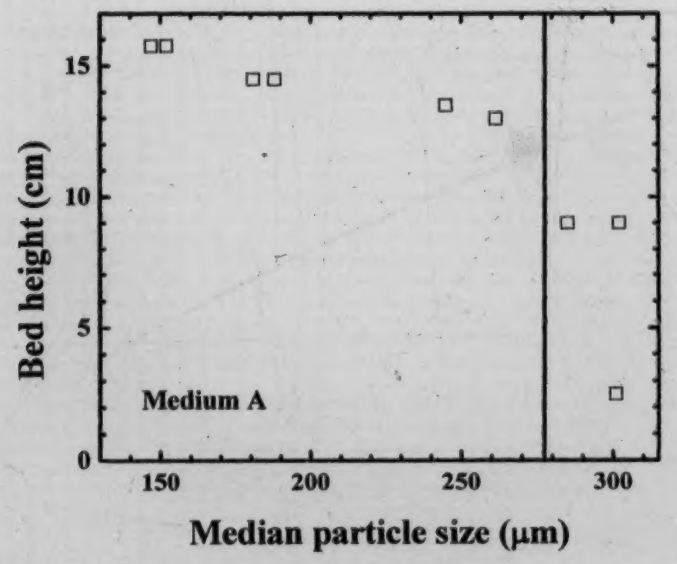


Figure 5-10. Median sizes of Medium A particles at various heights during fluidization.

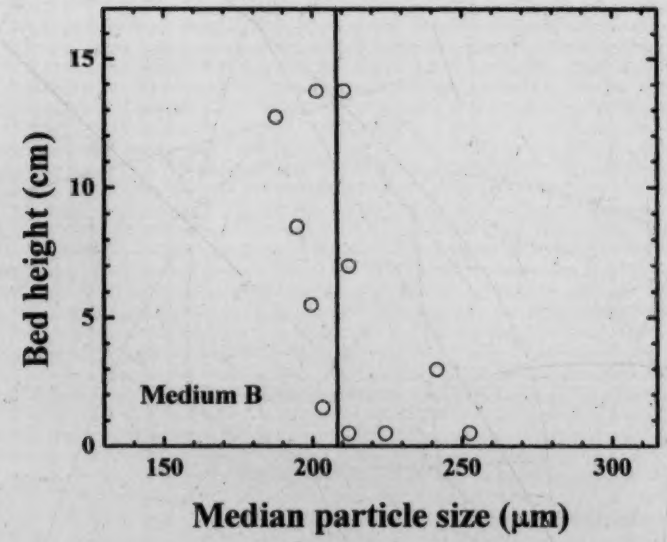


Figure 5-11. Median sizes of Medium B particles at various heights during fluidization.

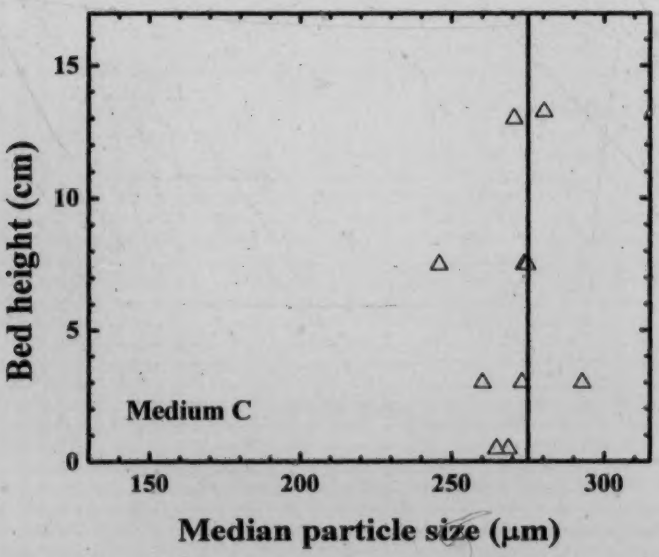


Figure 5-12. Median sizes of Medium C particles at various heights during fluidization.

As shown in Figure 5-10, the median size of Medium A particles increased dramatically with decreasing in bed height. This observation indicated a strong segregation of particles by size during fluidization, with finer medium particles at the top and coarser medium particles at the bottom. As shown by the fluidization classification diagram in Figure 4-3, coarser particles were of fluidization characteristics typical of a Geldart D solid. Such coarse particles were more difficult to fluidize than finer size particles. It was therefore concluded that the vertical transport of Medium A particles was weak during operation at the optimal fluidization velocity. In contrast, the median sizes of medium particles B and C were more uniform along the bed heights. From this observation, no conclusion could be made regarding the vertical transport of Medium B or Medium C particles during optimal separation.

## 5.4 *Separation efficiency evaluated at optimal fluidization air velocity*

During the experiments with the fluidization air velocity being optimized, ADMFB separation efficiency was evaluated by the relative closeness of the AMDFB separation result to the float-sink curve. To quantitatively evaluate the separation efficiency of the ADMFB for coal cleaning, the sharpness of separations ($E_p$) obtained using Media A, B and C at optimal fluidization air velocities were compared. A perfect density-based separation would have an $E_p$ value close to zero while a less efficient separation would have an increased $E_p$ value. The $E_p$ value of separating Seam 2 coal in 22.6x1.00 mm size fraction using the ADMFB was evaluated for the individual size

fractions of coal (22.6x5.66 mm, 5.66x3.36mm and 3.36x1.00 mm). The amount of coal added was equivalent to 6.7 vol.% of the medium particles at 15-cm packed bed height.

The experiments were conducted using the rapid shut off method, i.e. abruptly shutting off the inlet air during fluidization. It had been shown in this work that the ADMFB efficiency deteriorated with decreasing particle size of coal. For illustrative purposes, only the separation efficiencies of the coal in 3.36x1.00 mm size fraction using Media A, B and C were compared. The yield and ash content of the cleaned coal samples examined are given in Table 5-6.

Table 5-6. Yield and ash contents of cleaned coal samples collected in ADMFB separation experiments.

| Medium used | Size fraction (mm) | Yield (%) | Ash (%) |
|---|---|---|---|
| B | 22.6x5.66 | 68 | 10 |
| B | 5.66x3.36 | 71 | 11 |
| B | 3.36x1.00 | 74 | 15 |
| A | 3.36x1.00 | 74 | 15 |
| C | 3.36x1.00 | 57 | 15 |

Float-sink analysis was performed on each cleaned coal sample reported in the above table. Partition curves were generated to compare the separation efficiency achieved for coal of various size fractions and media tested. For each size fraction, the partition curve was constructed as the mass percentage of cleaned coal in a given density range with respect to the feed coal in the same density range. This mass percentage in each density range, known as partition coefficient, was then plotted against the corresponding average density. For more detailed information on the preparation of a

partition curve, please refer to Chapter 8 of Osborne's book entitled Coal Preparation Technology (1988). The partition curve for Seam 2 coal separated using Medium B at optimal fluidization air velocity is shown in Figure 5-13.

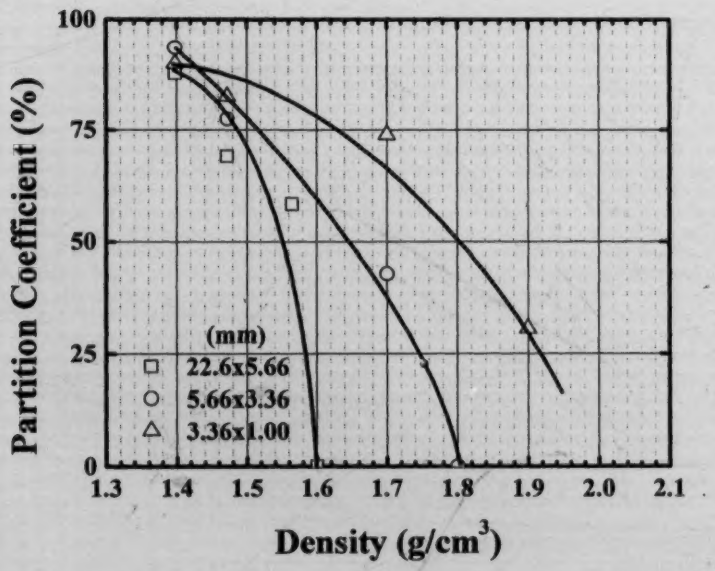


Figure 5-13. Partition curve for cleaned coal samples obtained using Medium B at optimal fluidization air velocity. Please refer to Appendix C for sample calculation.

Separation efficiency is generally characterized by the sharpness of separation ($E_p$). The calculation of $E_p$ is based on the *S.G.* difference at partition coefficients of 25% ($\rho_{25}$) and 75% ($\rho_{75}$). The calculation of $E_p$ is given as:

$$E_p = \frac{\rho_{25} - \rho_{75}}{2} \tag{5.1}$$

The smaller the value of $E_p$, the sharper the separation is. An $E_p$ value of 0.1 or lower is generally considered as an efficient separation (Luo et al., 2003).

The separation density ($\rho_{50}$) is the *S.G.* where partition coefficient is 50%. The $E_p$ and $\rho_{50}$ of coal in various size fractions using Medium A, Medium B and Medium C are given in Table 5-7.

Table 5-7. Separation efficiency of a 20-cm diameter ADMFB separator with Seam 2 coal.

| Medium used | Size fraction of coal (mm) | $E_p$* | $\rho_{50}$, ($\rho_{25} - \rho_{75}$) |
|---|---|---|---|
| B | 22.6x.5.66 | 0.05 | 1.55, (1.58 – 1.49) |
| B | 5.66x3.36 | 0.12 | 1.65, (1.75 – 1.52) |
| B | 3.36x1.00 | 0.15 | 1.81, (1.92 – 1.63) |
| A | 3.36x1.00 | 0.15 | 1.68, (1.83 – 1.53) |
| C | 3.36x1.00 | 0.21 | 1.80, (2.00 – 1.58) |

*Please refer to sample calculation in Appendix D.

When coal in size fraction of 22.6x1.00 mm was processed using the ADMFB, the $E_p$ value increased with decreasing particle size of coal. This observation indicated that the density separation by ADMFB was sharper for coarser coal. The $\rho_{50}$ value also increased with decreasing particle size of coal. This observation indicated that the separation density increased with decreasing particle size of coal when the coal of various size fractions was simultaneously separated in the same fluidized bed. Both of these observations support the conclusion that AMDFB separation efficiency decreased with decreasing particle size of coal.

The sharpness of separations for the coal in 3.36x1.00 mm size fraction were similar when processed with Medium A and Medium B as the separation medium; however, the $\rho_{50}$ obtained using Medium A was lower than that using Medium B. The

separation of the coal in 3.36x1.00 mm size fraction using Medium C was poor, as indicated by an $E_p$ value of 0.21. No strong correlation between the physical properties of the media and separation efficiency was observed.

From the $E_p$ values obtained for the coal of various size fractions, it was clear that ADMFB separation of coarser-sized coal was effective and not overly sensitive to the changes in process parameters. The ADMFB separations of the coal in 3.36x1.00 mm size fraction using Medium A and Medium B were similar. As shown by the $E_p$ value, the ADMFB separation efficiency was poorest when Medium C was used to form the separation medium.

It was clear that ADMFB separation was not a purely density-based separation process. This was shown by the differences in $\rho_{50}$ values obtained with the cleaned coal samples in various size fractions when Medium B was used. If ADMFB separation was a purely density-based separation, the $E_p$ and $\rho_{50}$ obtained for all size fractions of coal should be identical. Even though an optimal fluidization air velocity was identified to improve the separation of fine coals, the control (or mechanism) vertical transport of medium particles and the impact on density-based particle stratification remained unresolved.

Measurement of coal distribution during fluidization showed that the separation zone was mainly near the top for Medium A and throughout the fluidized bed for Medium B and Medium C. It was likely that the separation zone of each medium spanned a different density range.

## 5.5 *Effect of coal loading on ADMFB separation*

For practical purposes, it was important to determine the limit on the amount of coal that could be added to the fluidized bed for effective coal cleaning. The effect of coal loading on ADMFB separation was evaluated with the three media selected. The optimal fluidization air velocity determined previously for each medium was used for these ADMFB experiments. In the earlier experiments for determination of optimal fluidization air velocity, about 300 g of 22.6x1.00 mm coal was tested. In this set of tests, coal of the same size distribution at increasing amount (starting at 300 g) was added until the fluidized bed collapsed. The resulting separation was evaluated for the coal in 22.6x5.66 mm, 5.66x3.36 mm and 3.36x1.00 mm size fractions.

The amount of coal added was expressed as an apparent volume fraction of the initial packed bed of the medium particles. The particle size distribution of the 22.6x1.00 mm coal was given in Table 5-3. Only selected results were shown in order to demonstrate the effect of coal loading on separation efficiency. Using Medium B to process the coal in 22.6x1.00 mm size fraction, the effects of coal loading on the size-by-size separation efficiency at optimal fluidization air velocity are shown in Figures 5-14, 5-15 and 5-16 for the coal in 22.6x5.66 mm, 5.66x3.36 mm and 3.36x1.00 mm size fractions, respectively.

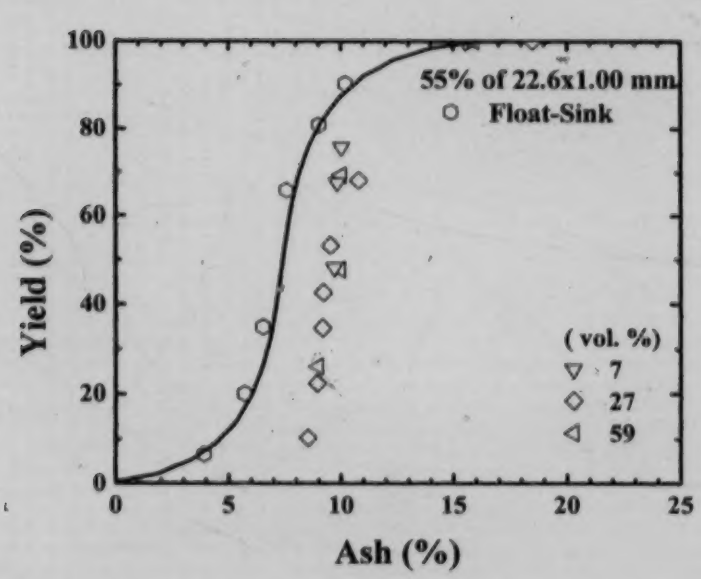


Figure 5-14. Effect of coal loading on ADMFB separation coal in 22.6x5.66 mm size fraction using Medium B.

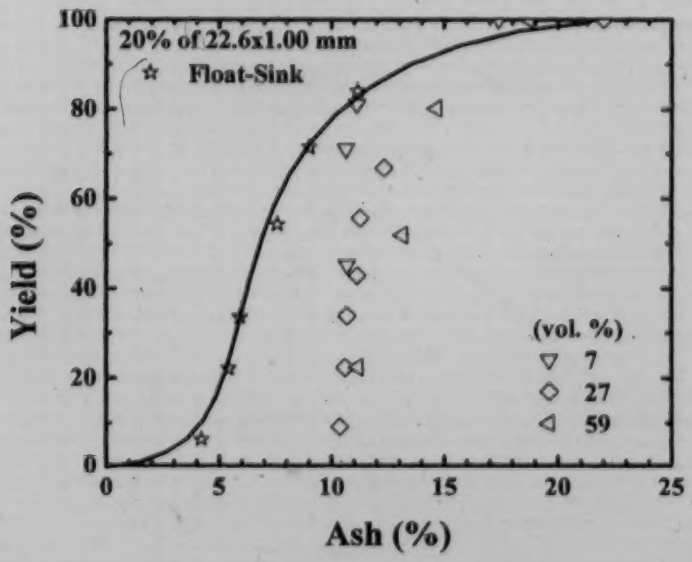


Figure 5-15. Effect of coal loading on ADMFB separation of coal in 5.66x3.36 mm size fraction using Medium B.

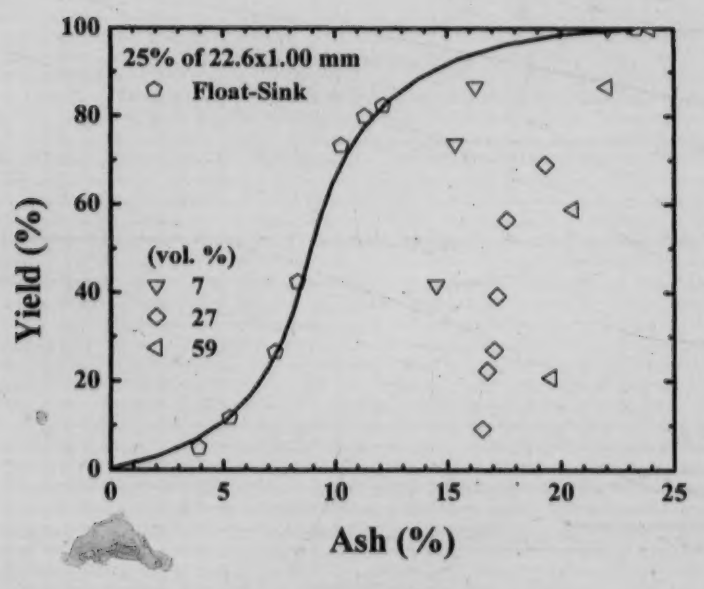


Figure 5-16. Effect of the coal loading on ADMFB separation of coal in 3.36x1.00 mm size fraction using Medium B.

The fluidized bed formed by Medium B collapsed upon coal equivalent to 59 % by volume of the initial packed bed height was added. The separation results of the coal in 22.6x5.66 mm size fraction, which corresponded to 55 wt.% of the 22.6x1.00 mm coal added, were insensitive to the volume of coal added to the fluidized bed up to 59 vol.%. At a yield of about 68%, ash reductions from 16% to 10% were obtained at both 7 vol.% and 59 vol.% coal additions.

In comparison of the results at 59 vol.% coal loading, shown in Figures 5-14, 5-15 and 5-16, the separation efficiency of finer coal (3.36x1.00 mm) deteriorated more significantly than the coarser coal. This was shown by a gradual shift in the results away from the corresponding float-sink curve with increasing in coal loading and decreasing particle size of coal. The results of coal separation at 7 vol.% coal loading for the coal in

the 3.36x1.00 mm size fraction showed an ash reduction from 23% to 15% at a 74% yield. In contrast, at 59 vol.% coal loading, an ash reduction from 23% to 19% was obtained at a yield of 69%, which represented a much less efficient separation. From the separation results of coal in the 22.6x1.00 mm size fraction, it was evident that the separation of finer coal (3.36x1.00 mm) was most susceptible to the volume of coal added to the fluidized bed.

The effect of coal loading on ADMFB separation was also tested with Media A and C. The results are shown in Figures 5-17 and 5-18 for the coal in 3.36x1.00 mm size fraction.

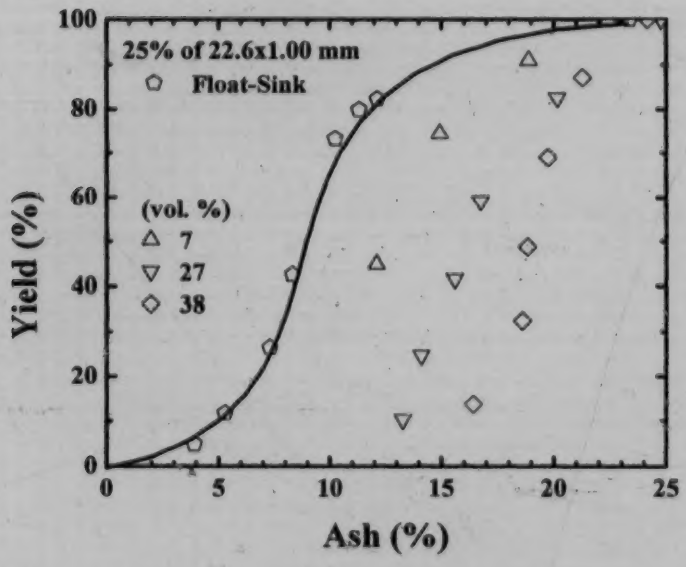


Figure 5-17. Effect of volume of coal added on ADMFB separation of coal in 3.36x1.00 mm size fraction using Medium A.

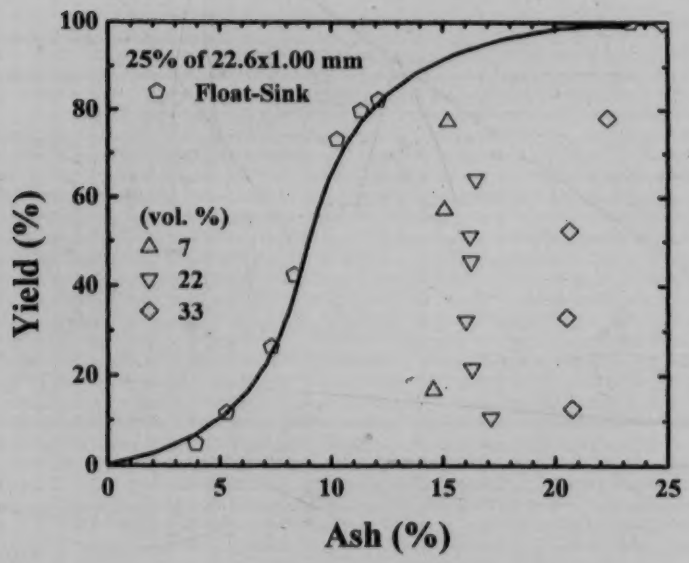


Figure 5-18. Effect of volume of coal added on ADMFB separation of coal in 3.36x1.00 mm size fraction using Medium C.

Separation results obtained using Media A and C as separation medium were similar to those obtained with Medium B. The ADMFB separation became less efficient as the volume of coal added to the fluidized bed increased. The maximum volume of the coal in 22.6x1.00 mm size fraction that could be added before the collapse of the fluidized bed was determined to be 38 vol.%, 59 vol.% and 33 vol.% of medium particles for Medium A, Medium B and Medium C, respectively. Of the media examined, Medium B had the smallest median particle size and lowest optimal fluidization air velocity. The separation medium formed by Medium B was observed to support the highest level of coal loading before the collapse of the fluidized bed.

Overall, it was observed that increasing coal loading would deteriorate ADMFB separation when the fluidization air velocity was fixed at the optimal value determined

previously. For a sufficiently high volume of coal addition, the coal added could possibly become the majority of the fluidized bed. It was known that the coal used in this study had a higher $u_{mb}$ than those of the media used. It was possible that the fluidization air velocity used for these tests could not support the volume of coal added, which caused the separation efficiency to deteriorate with increasing volume of coal added.

From the experiments with the 5-cm diameter ADMFB separator, the observed $u_{mb}$ for coal in 3.36x1.00 mm size fraction was 36.7 cm/s. This $u_{mb}$ was much greater than the optimal fluidization air velocities determined for the media used. As the volume of coal increased in the fluidized bed, it was expected that a higher fluidization air velocity would be needed to achieve a better separation. It was proposed that as the amount of coal added increased, the optimal separation would further resemble the separation in the pneumatic test.

## 5.6 *Effect of coal size on ADMFB separation*

In the ADMFB experiments to determine the optimal fluidization air velocity, the amount of coal added (300 g) only accounted for a small fraction of the fluidized bed. It was observed that at a constant fluidization air velocity, increasing the volume of coal added to the fluidized bed would decrease the separation efficiency. In this study, the coal in 22.6x1.00 mm size fraction was separated, and the separation results were evaluated on a size-by-size basis. After the separation, coal sample from each zone was split into three narrower size fractions (22.6x5.66 mm, 5.66x3.36mm and 3.36x1.00 mm) for closer examination. It was unclear whether the interaction of coals in different size

fractions would have an effect on their respective separation. To investigate this effect, the separation results of a selected size fraction with and without the presence of other size fractions were compared. In the first set of tests, 22.6x1.00 mm as-crushed coal particles were tested, and the separation was evaluated for the individual size fractions of coals. In the second set of tests, each size fraction of coal was tested individually. The separation results from these sets were then compared.

For the purpose of comparison, the volume of coal added in the respective size fraction tested was kept consistent between the sets of tests. The coals in 22.6x5.66 mm and 3.36x1.00 mm size fractions were used to demonstrate this effect. Medium B particles were used to form the separation medium and fluidized at the optimal fluidization air velocity given in Table 5-4. The results are shown in Figures 5-19 and 5-20.

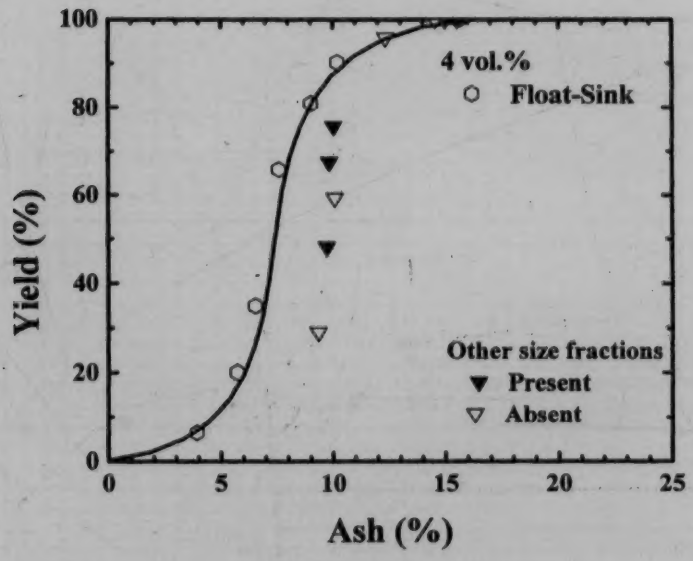


Figure 5-19. Effect of size fraction of coal added on ADMFB separation of coal in 22.6x5.66 mm size fraction using Medium B.

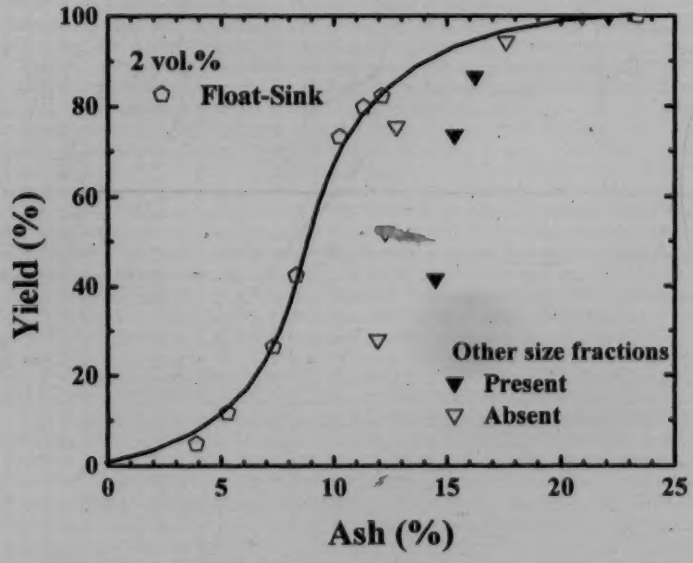


Figure 5-20. Effect of size fraction of coal added on ADMFB separation of coal in 3.36x1.00 mm size fraction using Medium B.

As shown in Figure 5-19, the presence of coals in other size fractions had no observable effect on the separation of coal in 22.6x5.66 mm size fraction. In contrast, Figure 5-20 showed that the presence of coarser coal had a signification effect on the separation of coal in 3.36x1.00 mm size fraction. An ash reduction from 23% to 15% was obtained at 74% yield when coal in 3.36x1.00 mm size fraction was separated as part of the 22.6x1.00 mm coal present (open triangle symbol). An improvement in ash reduction from 23% to 13% was obtained at 76% yield when the coal in 3.36x1.00 mm size fraction was separated individually. It was evident that the absence of coarser coal particles could improve the ADMFB separation efficiency of finer coal particles. The results also suggested that at the optimal fluidization air velocity, the ADMFB separation of the coal in 22.6x5.66 mm size fraction was at its optimal separation. This optimal separation could not be further improved by coal loading reduction with the fluidization system used.

From the observations made from the study on the effect of coal loading on ADMFB separation efficiency, it was obvious that the efficiency would improve in the absence of coal in other size fractions since the level of coal loading on the fluidized bed was decreased. However, the results on the separation efficiency of coal in 22.6x5.66 mm size fraction showed no improvement in the absence of coal in other size fractions. This observation indicated that a reduction in coal loading may not be the only cause of the improvement in separation efficiency seen with the 3.36x1.00 mm coal.

Another possible explanation for the improvement in ADMFB separation efficiency achieved with the coal in 3.36x1.00 mm size fraction was that the absence of larger coal particles minimized the vertical transport of medium particles. The

fluidization characteristics of coarser coals resembled that of Geldart D solids, which created large exploding bubbles upon fluidization. It was possible that as the amount of coarse coal particles increased, the vertical transport of medium particles would become more vigorous. Accordingly, the absence of coarser coals decreased the extent of back-mixing of finer coals during the fluidization. In order to improve the ADMFB separation efficiency for finer coal, narrow size distribution of feed coal and low level of coal loading were recommended. Further experiments were needed to distinguish the effects of coal loading and the presence of coarser coal particles on the separation efficiency of coal in 3.36x1.00 mm size fraction.

### 5.7 *Effect of bed height and fluidization duration on ADMFB separation*

In the previous experiments with the 20-cm diameter ADMFB separator, a packed bed height of 15 cm was used. The fluidization duration was fixed at 20 min. For engineering design purposes, it was essential to evaluate the effects of equipment dimension and residence time on ADMFB separation efficiency. To evaluate the effects of bed height and fluidization duration on ADMFB separation, 300 g of coal in the 22.6x1.00 mm size fraction was tested. Separation results of the coal in 3.36x1.00 mm size fraction were shown since this size fraction of coal was found to be the most sensitive to changes in process parameters.

The effect of fluidization duration on ADMFB separation efficiency at 15 min and 30 s were evaluated. The fluidization air velocity used for each medium was the average optimal velocity reported in Table 5-4 for 15-cm packed bed height. In addition, to

reduce the travel time needed for rejects particles to segregate, the packed bed height was reduced from 15 cm to 8 cm. The results are shown in Figures 5-21, 5-22 and 5-23.

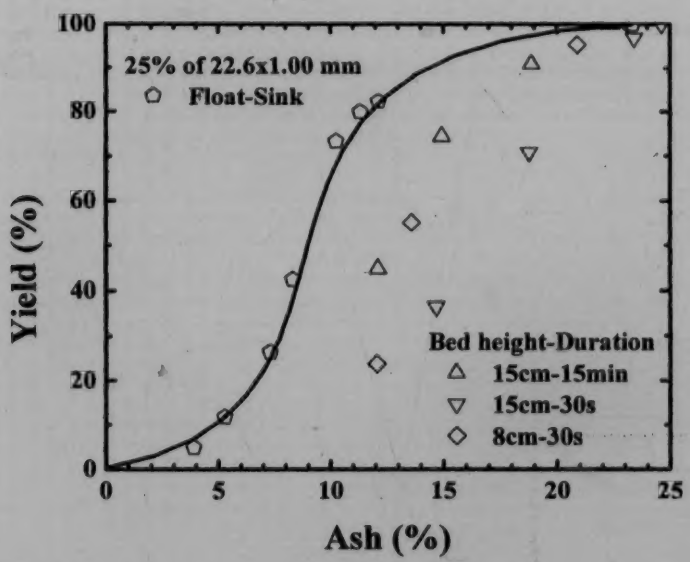


Figure 5-21. Effects of packed bed height and fluidization duration on ADMFB separation of coal in 3.36x1.00 mm size fraction using Medium A.

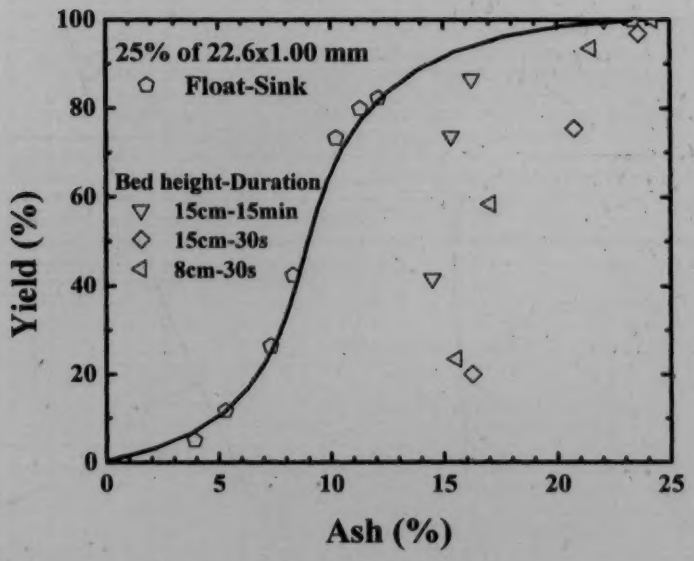


Figure 5-22. Effects of packed bed height and fluidization duration on ADMFB separation of coal in 3.36x1.00 mm size fraction using Medium B.

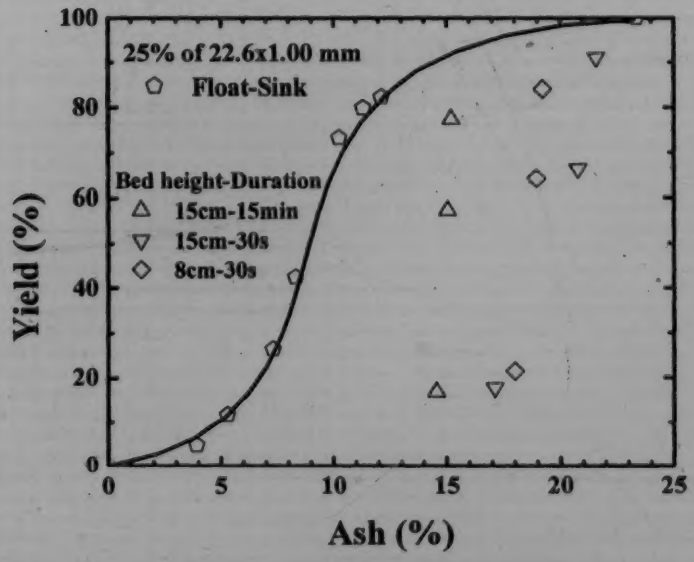


Figure 5-23. Effects of packed bed height and fluidization duration on ADMFB separation of coal in 3.36x1.00 mm size fraction using Medium C.

All three media studied showed a decrease in separation efficiency as the fluidization duration was decreased from 15 min to 30 s. The effects were shown by the shift of the experimental results further to the right from the float-sink curve. Upon decreasing the packed bed height from 15 cm to 8 cm at 30 s fluidization, separation efficiency was improved to an extent close to the optimal separation for Medium A. Decreasing the packed bed height also improved ADMFB separation for Medium B and Medium C when fluidization duration was also decreased from 15 min to 30 s. The improvements seen with Media B and C were less significant compared to that achieved with Medium A.

At a packed bed height of 15 cm, it was found that 30 s of fluidization duration was not sufficient to achieve optimal ADMFB separation for Medium A, Medium B or Medium C. When the packed bed height was decreased from 15 cm to 8 cm, 30 s of fluidization was sufficiently long for Medium A to achieve its optimal separation. The cumulative ash contents of coal samples collected from zones (from top to bottom) in the fluidized bed are shown in Figure 5-24.

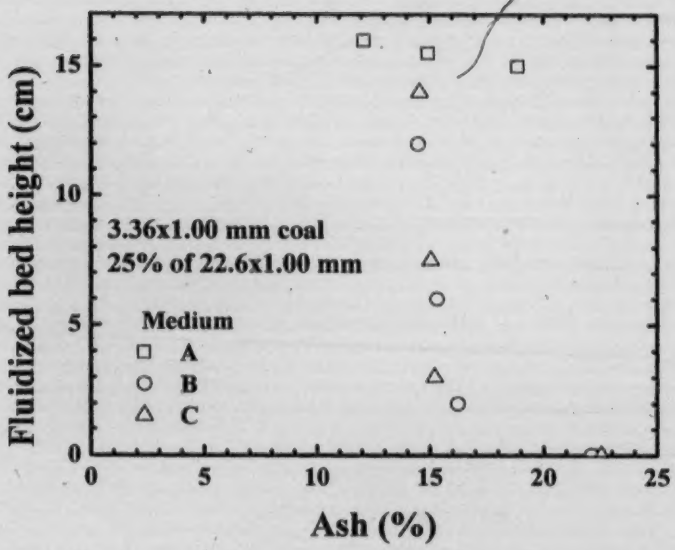


Figure 5-24. Ash content of coal particles in medium particles under optimal separation at 15-cm packed bed height and 15 min of fluidization duration.

The ash contents of the coal particles collected at the same fluidized bed height were different for various media tested. As shown in Figure 5-24 with Medium A, the ash content of the coal particles collected above the fluidized bed height of 15 cm was 19%, which was close to the feed ash content of 23%. In the case of Medium B and Medium C, the ash contents of the coal particles collected above the fluidized bed height of 5 cm maintained at approximately 15%. When either Medium B or Medium C was used, coal particles were distributed throughout the bed during fluidization. This observation was shown by the gradual increase in ash content of the coal particles collected with decreasing fluidized bed height.

The effective separation zone varied amongst the three media tested. Only a thin zone (between the surface and fluidized bed height of 15 cm) was utilized by Medium A

while most of the fluidized bed was utilized by Medium B and Medium C to achieve optimal separation. For coal particles separated in Medium B and Medium C, it was not surprise that optimal separation was not achieved in 30 s, as the rejects particles needed to travel deeper into the fluidized bed. Further experiments were needed to determine the suitable fluidization duration for optimal separation.

## 5.8 *Summary*

Three Geldart B media of different sizes and densities were used for ADMFB experiments in a 20-cm diameter column. An optimal fluidization air velocity was identified for each medium and was found to be applicable to various size fractions of coals examined with the fluidization system tested. The optimal separation efficiency was observed to decrease with decreasing particle size of coal. The separation of the coal in 3.36x1.00 mm size fraction was the most sensitive to the changes in operating parameters. Of the media used, the separation efficiency of the coal in 3.36x1.00 mm size fraction was lowest with Medium C. The ADMFB separation deteriorated with increasing amount of coal added. The separation suspension formed by Medium B supported the highest volume of coal before the fluidized bed collapsed. The separation of coal in 3.36x1.00mm size fraction improved when this coal was separated in the absence of coarser coal particles.

# CHAPTER 6 ASSOCIATION OF MERCURY AND MINERAL MATTERS IN COAL

From the ADMFB experiments, it had been shown that ADMFB was suitable as a separation process for coal cleaning of an Alberta sub-bituminous coal. One of the objectives of this study was to investigate whether the mercury contained in the coal studied could be rejected along with mineral matters rejection. To investigate this aspect, coal samples from various zones along the fluidized bed height in ADMFB were further classified into various size fractions and analyzed for ash content and mercury content. The correlations between ash content and mercury content for Seam 1 and Seam 2 coal are shown in Figures 6-1 and 6-2.

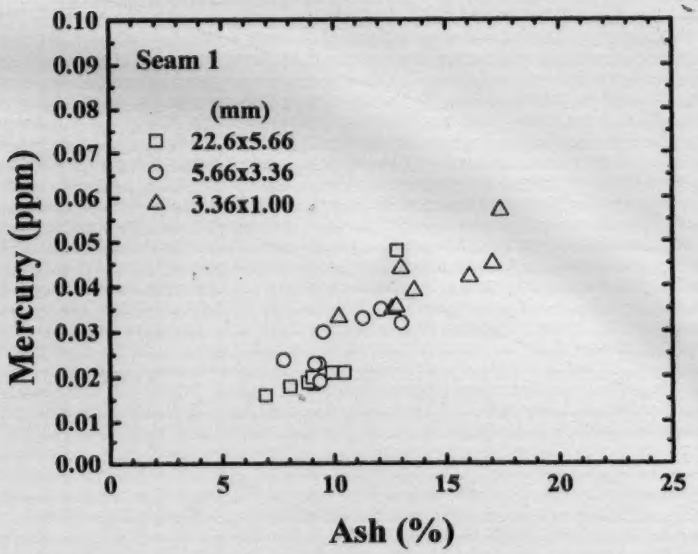


Figure 6-1. Relationship between ash content and mercury content for Seam 1 coal.

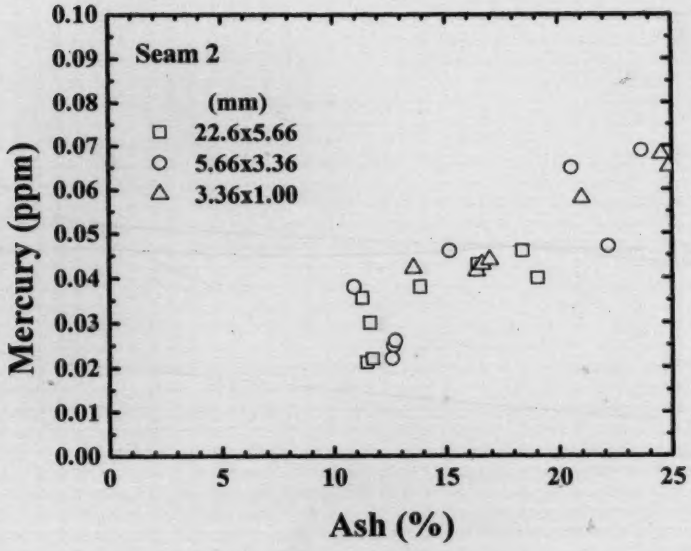


Figure 6-2. Relationship between ash content and mercury content for Seam 2 coal.

Figures 6-1 and 6-2 showed that the mercury content of the coal particles collected increased with increasing ash content with the two seams of coals used in this study. To demonstrate the potential of using an ADMFB for coal cleaning and mercury rejection, calculations of ash rejection and mercury rejection were performed according to the following formulae:

$$ash\ rejection = \frac{weight\ of\ ash\ in\ feed - weight\ of\ ash\ in\ cleaned\ coal}{weight\ of\ ash\ in\ feed} x100\% \quad (6.1)$$

$$mercury\ rejection = \frac{weight\ of\ mercury\ in\ feed - weight\ of\ mercury\ in\ cleaned\ coal}{weight\ of\ mercury\ in\ feed} x100\% \quad (6.2)$$

The correlation between ash rejection and mercury rejection for Seam 2 coal is shown in Figure 6-3.

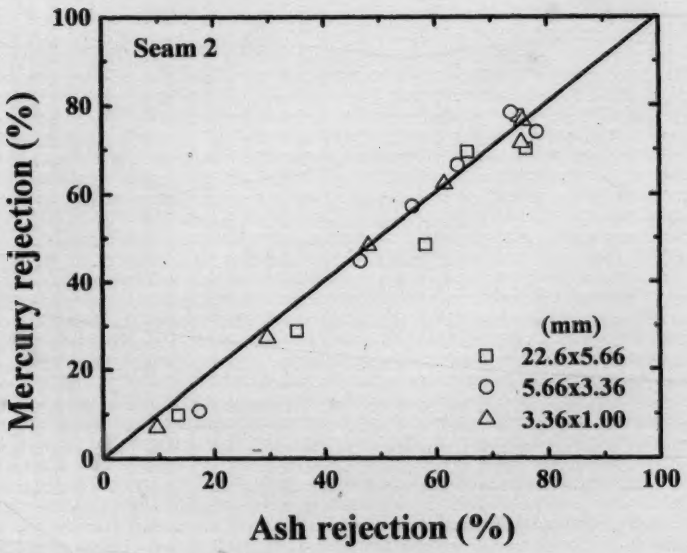


Figure 6-3. Correlation between ash rejection and mercury rejection for Seam 2 coal. Please see Appendix E for sample calculation.

A clear linear relationship between mercury rejection and ash rejection was evident in Figure 6-3. The above figure showed that this linear relationship between ash rejection and mercury rejection was applicable to all the size fractions of the coal examined in this study. This trend indicated that as the amount of ash-forming mineral matters removed from the feed coal increased, the amount of mercury removed from the feed coal would also increase linearly. The intercept of the trend line was close to zero. This observation suggested that mercury was heavily associated with the mineral matters in the coal. Upon cleaning two ranks of coal samples (bituminous and higher), López-Antón et al. (2006) also found that effective mercury removal from coal may be achieved by coal cleaning using a density-based separation method. Their results not only confirmed the association of mercury with mineral matters, but these results also

demonstrated potential mercury rejection via ash rejection by physical separations. With these results combined with the results in Figure 5-5 for Seam 2 coal in 22.6x5.66 mm size fraction, a 48% mercury removal at 72% combustible recovery was achievable by ADMFB separation (please refer to sample calculations in Appendix E). Combustible recovery was calculated according to the following formula:

$$combustible\ recovery = \frac{weight\ of\ combustible\ in\ cleaned\ coal}{weight\ of\ combustible\ in\ feed} x100\% \qquad (6.3)$$

Effective physical cleaning of finer-sized coal sizes would help further improve ash rejection and hence mercury rejection without sacrificing combustible recovery. The challenge was to effectively liberate mineral matters from coal at desired particle sizes suitable for various coal cleaning technologies.

# CHAPTER 7 CONCLUSIONS

From current study, the following conclusions could be derived.

- Coal finer than 1.00 mm could not be efficiently cleaned by ADMFB separation.
- Geldart B classified medium particles were suitable to form a bubbling fluidized bed for coal separation.
- For each medium studied, there was a narrow operating fluidization air velocity range where high coal separation efficiency could be achieved.
- Optimal fluidization air velocity was specific to the medium used for ADMFB separation.
- ADMFB separation efficiency decreased with increasing volume of coal added to the fluidized bed.
- The presence of coarser coal during fluidization deteriorated the separation efficiency of coal in 3.36x1.00 mm size fraction.
- The relationship between ash rejection and mercury rejection was linear with the sub-bituminous Seam 2 coal used in this study. This correlation showed the potential of mercury rejection from Alberta sub-bituminous coal by dry coal cleaning.

# CHAPTER 8 RECOMMENDATIONS

It was found that an optimal fluidization air velocity for optimal separation existed for the media studied. It was proposed that the vertical transport of medium particles was low during this optimal separation. Monitoring of the vertical transport of medium particles during optimal separation was needed to verify this suspicion.

Results of studies of mercury rejection and ash rejection suggested a clear association of mercury with mineral matters in the coal studied. Further work was needed to identify the mineral phases that bound specifically with mercury. If possible, different mineral phases should be isolated and further evaluated for mercury association.

**REFERENCES**

Akers, D. and R. Dospoy, "Role of Coal Cleaning in Control of Air Toxics," Fuel Processing Technology **39(1-3)**, 73-86 (1994).

Andreux, R., T. Gauthier, and O. Simonin, "New Description of Fluidization Regimes," American Institute of Chemical Engineers Journal **51**, 1125-1530 (2005).

Anjaneyula, P. and D. V. Khakhar, "Rheology of a Gas-Fluidized Bed," Powder Technology **83(1)**, 29-34 (1995).

ASTM International, "Section 05 Petroleum Products, Lubricants, & Fossil Fuels," in "ANNUAL BOOK OF ASTM STANDARDS 2005," Dr. M. R. Mitchell, Ed., West Conshohocken, PA (2005).

Beauchamp, R., "Modified Coal Digestion and Mercury Analysis Procedure," Department of Chemical and Materials Engineering, University of Alberta, (2006).

Carey, T., R. Chang, F. Meserole, M. Rostam-Abadi, and S. Chen, "Assessing Sorbet Injection Mercury Control Effectiveness in Flue Gas Streams," Environmental Progress **19(3)**, 167-174 (2000).

Chen, Q. and Y. Yang, "Development of Dry Beneficiation of Coal in China," Coal Preparation **23**, 3-12 (2003).

Choung, J., C. Mak, and Z. Xu, "Fine Coal Beneficiation using an Air Dense Medium Fluidized Bed," Coal Preparation **26**, 1-15 (2006).

Collot, A., "Matching Gasification Technologies to Coal Properties," International Journal of Coal Geology **65**, 191-212 (2006).

Crock, J. G., "Determination of Total Mercury in Biological and Geological Samples," U.S. Geological Survey. http://pubs.usgs.gov/of/2005/1030/pdf/OFR2005_1030_508.pdf (accessed 12/06, 2006).

Dahl, S. R. and C. M. Hrenya, "Size Segregation in Gas-Solid Fluidized Beds with Continuous Size Distributions," Chemical Engineering Science **60**, 6658-6673 (2005).

Dechsiri, C., Van der Zwan, E.A., H. G. Dehling, and A. C. Hoffmann, "Dispersion of Particle Pulses in Fluidized Beds Measured by Positron Emission Tomography," American Institute of Chemical Engineers Journal **51(3)**, 791-801 (2005).

Delebarre, A. B., J. Morales, and L. Ramos, "Influence of the Bed Mass on its Fluidization Characteristics," Chemical Engineering Journal **98**, 81-88 (2004).

Delebarre, A. B., A. Pavinato, and J. C. Leroy, "Fluidization and Mixing of Solids Distributed in Size and Density," Powder Technology **80**, 227-233 (1994).

Environment Canada, "Mercury and the Environment," http://www.ec.gc.ca/mercury/en/index.cfm (accessed 05/05, 2006).

Geldart, D., "Gas Fluidization Technology," John Wiley and Sons Ltd., Chichester, NY (1986).

Geldart, D., "Types of Gas Fluidization," Powder Technology **7(5)**, 285-292 (1973).

Goodarzi, F., "Speciation and Mass-Balance of Mercury from Pulverized Coal Fired Power Plants Burning Western Canadian Subbituminous Coals," The Journal of Environmental Monitoring Focuses on Environmental Processes and Impacts **6**, 792-798 (2004).

Goyer, R. A., "Casarett and Doull's Toxicology: The Basic Science of Poisons. 4th ed.," Pergamon Press, New York, USA (1991).

Hetsroni, G., "Handbook of Multiphase Systems," G. Hetsroni, Ed., Hemisphere, New York, USA (1982).

Jin, H., Z. Tong, H. I. Schlaberg, and J. Zhang, "Separation of Fine Binary Mixtures under Vibration in a Gas-Solid Fluidized Bed with Dense Medium," Waste Management and Research **23**, 534-540 (2005).

Jin, H., Z. Tong, J. Zhang, and B. Zhang, "Homogeneous Fluidization Characteristics of Vibrating Fluidized Beds," The Canadian Journal of Chemical Engineering **82**, 1048-1053 (2004).

Kileijin van Willigen, F., J. R. van Ommen, J. van Turnhout, and C.M. van den Bleek, "Bubble Size Reduction in Electric-Field-Enhanced Fluidized Beds," Journal of Electrostatics **63**, 943-948 (2005).

Kunii, D. and O. Levenspiel, "Fluidization Engineering SECOND EDITION," Butterworth-Heinemann, Newton, MA (1991).

Long, S. E. and W. R. Kelly, "Determination of Mercury in Coal by Isotope Dilution Cold-Vapor Generation Inductively Coupled Plasma Mass Spectrometry," Analytical Chemistry **74(4)**, 1477-1483 (2002).

Lopex-Anton, M. A., M. Diaz-Somoano, A. B. Gracia, and M. R. Martinex-Tarazona, "Evaluation of Mercury Association in Two Coals of Different Rank using Physical Separation Procedures," Fuel **85**, 1389-1395 (2006).

Lu, G., [Personal Communication], (2006).

Luo, Z., Y. Zhao, Q. Chen, X. Tao, and M. Fan, "Separation Lower Limit in a Magnetically Gas-Solid Two-Phase Fluidized Bed," Fuel Processing Technology **85**, 173-178 (2003a).

Luo, Z., Y. Zhao, X. Tao, M. Fan, Q. Chen, and L. Wei, "Progress in Dry Coal Cleaning using Air-Dense Medium Fluidized Beds," Coal Preparation **23**, 13-20 (2003b).

Marzocchella, S. and P. Salatino, "Fluidization of Solids with $CO_2$ at Pressures from Ambient to Supercritical," American Institute of Chemical Engineers Journal **46(5)**, 901-910 (2000).

Merry, J. M. D. and J. F. Davidson, "Gulf-Stream Circulation in Shallow Fluidized-Beds," Transactions of the Institution of Chemical Engineers **51**, 361-368 (1973).

Osborne, D. G., "Coal Preparation Technology," Graham and Trotman Limited, Oxford, Great Britain (1988).

Oshitani, J., K. Ono, M. Ijiri, and Z. Tanaka, "Effect of Particle Fluidization Intensity on Floating and Sinking of Objects in a Gas-Solid Fluidized Bed," Advanced Powder Technology **15(2)**, 201-213 (2004).

P S Analytical, "MAINTENANCE AND SERVICE PROCEDURES," http://www.psanalytical.com/Online%20service%20procedures.htm (accessed 16/07, 2006).

Peng, F. F., Q. Dai, and D. C. Yang, "Analysis of Packed Column Jig for Fine Coal Separation," Coal Preparation **22**, 199-217 (2002).

Rees, A. C., J. F. Davidson, J. S. Dennis, and A. N. Hayhurst, "The Rise of a Buoyant Sphere in a Gas-Fluidized Bed," Chemical Engineering Science **60**, 1143-1153 (2005).

Rowe, P. N. and B. A. Partridge, "Proc. Symp. Interaction between Fluids and Particles," Institute of Chemical Engineers, 135 (1962).

Sasongko, D. and J. Stubington, "Significant Factors Affecting Devolatilization of Fragmenting, Non-Swelling Coals in Fluidized Bed Combustion," Chemical Engineering Science **51(16)**, 3909-3918 (1996).

Sidorenko, I. and M. J. Rhodes, "Influence of Pressure on Fluidization Properties," Powder Technology **141(1-2)**, 137-154 (2004).

Umekawa, H., S. Furui, Y. Oshima, M. Okura, M. Ozawa, and N. Takenaka, "Quantitative Measurement of Segregation Phenomena in a Binary-Mixture Fluidized Bed by Neutron Radiography," Nuclear Instruments and Methods in Physics Research A **542**, 219-225 (2005).

Wen, C. Y. and Y. H. Yu, "A Generalized Method for Predicting Minimum Fluidization Velocity," American Institute of Chemical Engineers Journal **12**, 610 (1966).

Xu, S. and Y. Guan "Numerical Simulation and Experimental Validation of Magnetic Media Performance in Air-Dense Medium Fluidized Bed," Coal Preparation **23**, 57-65 (2003).

Xu, Z., "ADVANCED COAL CLEANING AND COMBUSTION TECHNOLOGY: PROGRESS REPORT 2," Department of Chemical and Materials Engineering, University of Alberta: NSERC/EPCOR/AERI Industrial Research Chair, (2003).

# APPENDICES

## *Appendix A*

This appendix contains the modified procedure for coal digestion and mercury analysis.

A modified procedure of the Test Method ASTM 6414-01: Coal digestion and Mercury Analysis was followed. The modified procedure for coal digestion and mercury is shown below (Beauchamp, 2006; Crock, 2005; and Lu, 2006).

### 1. Digestion

1. Soak all glassware in 10% $HNO_3$ at least 48 hours and rinse well with DI water before use
2. Add 0.1000 ± 0.0009 g $V_2O_5$ (as received) to 16 mm x 150 mm disposable glass culture tube
3. Add 0.1500 ± 0.0009 g of -250μm coal to the tube, shake the tube gently to mix.
    - Prepare 2 tubes from each coal sample to ensure consistent results
    - Prepare a blank (no coal) identically to the samples
4. Pipette 10 drops (standard disposable pipette) of anhydrous ethanol to each tube
5. Pipette 3.5 mL $HNO_3$ (68-70% assay, SG 1.42, Baker Instra-analyzed) to each tube as follows:
    - 2 rounds of 0.25 mL per tube

- 2 rounds of 0.50 mL per tube
- 2 rounds of 1.00 mL per tube

6. Swirl tubes gently, cover with watch glass, and allow mixture to react at room temperature for 1 hour
7. Add 1.5 mL $H_2SO_4$ (Concentrated, SG 1.83, FCC grade from Fisher or Baker Instra-analyzed ) to each tube, swirl tubes to mix – the mixture appear to be black
8. Cover tubes with watch glass, ramp temperature in heating block to $150^0$C over 2 hours
9. Maintain at $150^0$C for 16 hours
10. Cool to $50^0$C at ambient conditions – the mixture is now rusty-red
11. Carefully add 2 mL $H_2O_2$ (30% v/v) to each tube, 0.25 mL at a time – the mixture is now dark green
12. Swirl tubes, cover and reheat the mixture to boil for 5 minutes (~$150^0$C)
13. Cool tubes to room temperature
14. Dilute the mixtures to 25 mL using ultra-pure DI water – the mixture is now light green
15. Cap and store the diluted samples (max. 1 week) for Hg analysis. Ensure that all solids in the samples have settled prior to analysis.

## 2. Hg analysis – cold vapour atomic fluorescence spectrometry (PSA 10.035 Millennium Merlin/Galahad System, P S Analytical, England)

1. To each tube, add 2 drops of $KMnO_4$ (5g/100 mL water), wait 2 minutes, and then swirl gently until the color red disappears. Add 1.25 mL hydroxylamine hydrochloride to each tube ($NH_2OH$-HCl, 1.5g/100 mL water). Swirl the tube gently. Samples must be analyzed within 1 hour [3].
2. Prepare Hg calibration standards
3. Prepare reductant solutions – 25 % m/v $SnCl_2 \cdot 2H_2O$ in 20 %v/v HCl solution.
    - Dissolve $SnCl_2$ in concentrated HCl – heat the solution to ~$50^0$C while, mixing the solution until all the solids are dissolved
    - Allow the acid solution to cool to room temperature, then carefully dilute the solution with DI water
    - Purge the solution with argon gas for 24 hours to remove traces of Hg
4. Prepare blank/cleaning solution – 5% v/v HCl + 5% v/v $HNO_3$.
5. Analyze samples as per PSA user's manuals.
6. NOTE: every $6^{th}$ sample should be the blank to monitor zero baseline drift

## 3. Calculations

Let the Hg concentrations obtained above be Measured values (ppb), then:

Corrected value (ppb) = Measured value (ppb) – Measured value for blanks (ppb)

Mercury in sample (ppm) is:

$$\text{Hg in sample (ppm)} = \text{Corrected value (ppb)} \times \frac{1\,\mu\text{g/L}}{1\,\text{ppb}} \times \frac{0.02625^{*}\ \text{L sol'n}}{\text{x g coal}} [=] \frac{\mu\text{g Hg}}{\text{g (coal + Hg)}} [=] \text{ppm}$$

0.025 L diluted digest solution + 0.00125 L $NH_2OH$-HCl = 0.02625 L solution

***Appendix B***

This section contains the sample calculation for the $u_{mf}$ values reported in Table 5-1.

Table B-1. Values used for calculation of $u_{mf}$ using a 20-cm diameter ADMFB separator.

| Medium | Weight (g) | Density ($g/cm^3$) | $d_p$ (cm) | $\phi_s$* | $h_{mf}$** (cm) | $u_{mf}$ (cm/s) | $Re$ |
|---|---|---|---|---|---|---|---|
| A | 11970.6 | 4.8 | 0.0278 | 0.58 | 15.2 | 9.4 | 2.19 |
| B | 8223.1 | 3.5 | 0.0208 | 0.58 | 15.5 | 5.4 | 0.687 |
| C | 7236.2 | 2.7 | 0.0262 | 0.86 | 15.5 | 7.8 | 1.04 |

*Values adapted from Kunii and Levenspiel, 1991.

**Values obtained from Figures 5-2, 5-3 and 5-4.

$\varepsilon_{mf}$ was estimated from the $h_{mf}$ value as follow:

$$\varepsilon_{mf} = 1 - \frac{volume\ of\ medium}{volume\ of\ fluidized\ bed\ at\ minimum\ fluidization} \qquad (B.1)$$

$$\varepsilon_{mf} = 1 - \frac{\frac{weight\ of\ medium}{density\ of\ medium}}{\frac{1}{4} * d^2 * \pi * h_{mf}}$$

$$\varepsilon_{mf} = 1 - \frac{\frac{11970.6g}{4.79g/cm^3}}{\frac{1}{4} * (20cm)^2 * \pi * 15.2cm}$$

$$\varepsilon_{mf} = 0.477$$

$$u_{mf} = \frac{d_p^2(\rho_s - \rho_g)g}{150\mu} \frac{\varepsilon_{mf}^3 \varphi_s^2}{1-\varepsilon_{mf}}, \quad Re_{p,mf} < 20 \tag{2.1}$$

$$u_{mf} = \frac{(0.0278cm)^2 * (4.79 - 0.0012)g/cm^3 * 981cm/s^2}{150 * 0.00018g/cm \cdot s} \frac{(0.477)^3 * (0.58)^2}{1-0.477}$$

$$u_{mf} = 9.36cm/s$$

For Equation 2.1 to be valid, $Re_{p,mf}$<20

$$Ar = \frac{d_p^3 \rho_g (\rho_s - \rho_g)g}{\mu^2} \tag{2.3}$$

$$Ar = \frac{(0.0278)^3 * 0.0012 * (4.79 - 0.0012) * 981}{0.00018^2}$$

$$Ar = 3738$$

The equation for $Re_{p,mf}$ is given as

$$Re_{p,mf} = [(33.7)^2 + 0.0408Ar]^{1/2} - 33.7 \tag{2.2}$$

$$Re_{p,mf} = [(33.7)^2 + 0.0408 * 3738]^{1/2} - 33.7$$

$$Re_{p,mf} = 2.19$$

Since $Re_{p,mf}$<20, the usage of Equation 2.1 is valid.

***Appendix C***

This section contains the procedure followed for the generation of partition curve shown in Figure 5-13.

Table C-1. Float-sink analysis of feed and cleaned coal in 22.6x5.66 mm size fraction.

| | Feed | Cleaned coal | | |
|---|---|---|---|---|
| Density ($g/cm^3$) | Weight* (%) | Weight* (%) | Weight** (%) | Partition coefficient (%) |
| 1.38-1.41 | 25.6 | 22.5 | 33.3 | 87.8 |
| 1.41-1.53 | 52.5 | 36.3 | 53.7 | 69.1 |
| 1.53-1.60 | 1.6 | 0.9 | 1.4 | 58.5 |
| 1.60-1.80 | 10.7 | 0.0 | 0.0 | 0.0 |
| Total | 90.4 | 59.7 | 88.4 | - |

*Percent of feed (%).

**Percent of cleaned coal (%).

$$Partition\ coefficient\ of\ cleaned\ coal = \frac{amount\ of\ cleaned\ coal\ in\ a\ certain\ density\ range}{amount\ of\ feed\ in\ a\ certain\ density\ range} \quad (C.1)$$

$$Partition\ coefficient\ of\ cleaned\ coal\ (1.38\ g/cm^3\text{-}1.41\ g/cm^3) = \frac{59.7 * \frac{33.3}{88.4}}{25.6}$$

$$Partition\ coefficient\ of\ cleaned\ coal\ (1.38\ g/cm^3\text{-}1.41\ g/cm^3) = 87.8\%$$

***Appendix D***

This section contains the sample calculation for the $E_p$ values reported in Table 5-7.

Coal in 22.6x5.66 mm size fraction was used. From Figure 5-13, the partition coefficient at 25%, 50% and 75% is reported in the following table.

Table D-1. Values used for calculation of $E_p$ of a cleaned coal sample in 22.6x5.66 mm size fraction.

| Medium | Coal size fraction (mm) | $\rho_{25}$ | $\rho_{50}$ | $\rho_{75}$ |
|---|---|---|---|---|
| B | 22.6x5.66 | 1.58 | 1.55 | 1.49 |

$$E_p = \frac{\rho_{25} - \rho_{75}}{2} \tag{5.1}$$

$$E_p = \frac{1.58 - 1.49}{2}$$

$$E_p = 0.05$$

***Appendix E***

The section contains the sample calculations performed for the ash rejection and mercury rejection and the combustible recovery values reported in Chapter 6.

Coal in 22.6x5.66 mm size fraction was used. The yield, ash content and mercury content of the cleaned coal sample discussed is given in the following table..

Table E-1. Values used for calculation of ash rejection, mercury rejection and combustible recovery of a cleaned coal sample in 22.6x5.66 mm size fraction.

| Feed coal | | Cleaned coal | | |
|---|---|---|---|---|
| Ash (%) | Mercury (ppm) | Yield (%) | Ash (%) | Mercury (ppm) |
| 16 | 0.040 | 69 | 12 | 0.030 |

$$ash\ rejection = \frac{weight\ of\ ash\ in\ feed - weight\ of\ ash\ in\ cleaned\ coal}{weight\ of\ ash\ in\ feed} x100\%$$

(6.1)

$$ash\ rejection = \frac{16 - 69*(12/100)}{16} x100\%$$

$$ash\ rejection = 48\%$$

$$mercury\ rejection = \frac{weight\ of\ mercury\ in\ feed - weight\ of\ mercury\ in\ cleaned\ coal}{weight\ of\ mercury\ in\ feed} x100\%$$

(6.2)

$$mercury\ rejection = \frac{0.040\times10^{-6}*100 - 69*0.030\times10^{-6}}{0.040\times10^{-6}} x100\%$$

$$mercury\ rejection = 48\%$$

$$combustible\ recovery = \frac{weight\ of\ combustible\ in\ cleaned\ coal}{weight\ of\ combustible\ in\ feed} x100\% \quad (6.3)$$

$$combustible\ recovery = \frac{69*((100-12)/100))}{(100-16)} x100\%$$

$$combustible\ recovery = 72\%$$